STELIB: a library of stellar spectra at R∼2000 ⋆

J.-F. Le Borgne[1], G. Bruzual[2], R. Pelló[1], A. Lançon[3], B. Rocca-Volmerange[4], B. Sanahuja[5], D. Schaerer[1], C. Soubiran[6], R. Vílchez-Gómez[7]

[1] Laboratoire d'Astrophysique (UMR 5572), Observatoire Midi-Pyrénées, 14 Avenue E. Belin, F-31400 Toulouse, France
[2] Centro de Investigaciones de Astronomía, AP 264, 5101-A Mérida, Venezuela
[3] Observatoire de Strasbourg (UMR 7550), 11 rue de l'Université, F-67000 Strasbourg, France
[4] Institut d'Astrophysique de Paris (UMR 7095), 98 bis Boulevard Arago, F-75014 Paris, France
[5] Departament d'Astronomia i Meteorologia, Universitat de Barcelona, Martí i Franquès 1, E-08028 Barcelona, Spain
[6] Observatoire de Bordeaux, (UMR 5804), BP 89, F-33270 Floirac, France
[7] Departamento de Física, Universidad de Extremadura, Avda. de la Universidad, s/n E-10071 Cáceres, Spain

re-submitted version 10 February 2003

Abstract. We present STELIB, a new spectroscopic stellar library, available at http://webast.ast.obs-mip.fr/stelib. STELIB consists of an homogeneous library of 249 stellar spectra in the visible range (3200 to 9500Å), with an intermediate spectral resolution ($\lesssim$3Å) and sampling (1Å). This library includes stars of various spectral types and luminosity classes, spanning a relatively wide range in metallicity. The spectral resolution, wavelength and spectral type coverage of this library represents a substantial improvement over previous libraries used in population synthesis models. The overall absolute photometric uncertainty is 3%.

Key words. atlases - stars: fundamental parameters - galaxies: stellar content.

1. Introduction

Evolutionary population synthesis models that describe the chemical and spectral evolution of stellar systems in detail are fundamental tools in the analysis of observations of both nearby and distant galaxies (e.g. Guiderdoni & Rocca-Volmerange 1987, Buzzoni 1989, Bruzual & Charlot 1993, Fioc & Rocca-Volmerange 1997). They are needed to determine the stellar populations in a variety of systems, spanning a wide range of metallicities, from early type galaxies and spiral bulges to star forming galaxies at different redshifts.

The possibility of building detailed spectro-chemical evolution models of stellar populations using evolutionary synthesis techniques is limited by the lack of comprehensive empirical libraries of stellar spectra, comprising stars with metallicities ranging from well below solar ([Fe/H] from -2 to -1) to above solar ([Fe/H]>0). Direct inversions of galaxy spectra (Pelat 1997, Boisson et al. 2000) are also handicaped by this shortage. Current synthesis models based on empirical stellar data are mostly restricted to solar metallicity. In the visible range, they are largely based on the spectral atlas of Gunn & Stryker (1983) or the more recent (and not completely independent) atlas of Pickles (1998).

The use of theoretical stellar spectra such as Kurucz' (1992) instead of empirical libraries is *a priori* preferable, because they can be computed for a dense grid of fundamental parameters (metallicity, gravity, effective temperatures), thus avoiding interpolation errors and calibrations. However, the resulting synthetic spectra do not in general reproduce the spectral features observed in composite stellar populations with the same degree of accuracy as models based solely on observed stellar spectra. Methods to achieve photometric compatibility between models and data have been developed (Lejeune et al. 1997), and extended and homogeneous libraries of theoretical spectra covering the bulk of the HR-diagram and a wide range of metallicities are now available (Lejeune

Send offprint requests to: J.-F. Le Borgne, leborgne@ast.obs-mip.fr

⋆ Based on observations collected with the Jacobus Kaptein Telescope, (owned and operated jointly by the Particle Physics and Astronomy Research Council of the United Kingdom, the Nederlandse Organisatie voor Wetenschappelijk Onderzoek of the Netherlands and the Instituto de Astrofsica de Canarias of Spain and located in the Spanish Observatorio del Roque de Los Muchachos on La Palma which is operated by the Instituto de Astrofsica de Canarias), the 2.3m telescope of the Australian National University at Siding Spring, Australia, and the VLT-UT1 Antu Telescope (ESO).

et al. 1998, Westera et al. 2002). While this represents a major improvement, such libraries still suffer from the limited resolution (∼20Å in the optical). The determination of stellar populations in galaxies up to z∼1 through optical spectroscopy requires spectral synthesis capabilities over a broad wavelength range (∼3000Å to ∼1,μm). A minimum spectral resolution of a few Å is necessary to obtain constraints on age, metallicity and global stellar kinematics from absorption lines. The libraries presently available with a suitable spectral resolution (1-3Å) are often limited to a narrow wavelength range (Jones 1997, Cenarro et al. 2001) or are restricted to particular spectral types (Montes et al. 1999).

The main objective of our stellar library STELIB is to provide a homogeneous set of stellar spectra in the visible range (3200 to 9500Å), with a relatively high spectral resolution ($\lesssim$3Å) and sampling (1Å). This library includes stars of most spectral types and luminosity classes and spans a relatively wide range in metallicity. Most of the stars in our sample have measured metallicities.

The outline of the paper is the following. In Section 2 we present the observations. Section 3 describes the selection criteria and the overall characteristics of the STELIB sample of stars. The data reduction process is summarized in Section 4. Section 5 presents the content of the library STELIB, presently available through the web. In Section 6 we show some particular applications of STELIB to population synthesis studies, and we compare the performances of this library to previous results. The conclusions of this paper are given in Section 7.

2. Observations

The data were obtained during two runs, one at the 1m Jacobus Kaptein Telescope (JKT), Roque de los Muchachos Observatory, La Palma, Canary Islands, Spain, between 1994 March 28 and April 4, and a second one at the 2.3m of the Australian National University at Siding Spring (SSO), Australia, between 1994 December 25 and 31. On JKT, we used the Richardson-Brealey Spectrograph with the 600 lines/mm grating. The detector was a EEV7 1242×1152 CCD with a 22.5μm pixel. The slit width was 1.5 arcsec. This configuration gives a dispersion of 1.7Å/pixel and a resolution of about 3Å FWHM. We made use of both blue and red optics. With the blue optics, spectra were alternatively obtained with 2 grating angle settings: 18°giving a wavelength range of 2900Å-5100Å on the CCD (useful data start at ∼3200Å because of atmospheric cutoff) and 21°giving the wavelength range 4300Å-6500Å. With the red optics the grating angle settings were 24°and 27°for the wavelength ranges 6000Å-8200Å and 7600Å-9900Å, respectively. To maximize the efficiency, and to improve the calibration, each night was devoted to a single grating angle setting: changing the grating angle was done manually by opening the spectrograph. March 29 was an exception because 2 settings with the red optics were used (see Table 1 for details). Again to save time, the spectrograph was not rotated to align the slit on the paralactic angle, since it should have to be done manually on the telescope for each pointing. This should have no consequence because of the relatively short wavelength range of each individual spectra, the slit width of 1.5 arcsec, and also because we observed as close to the meridian as possible (the slit was set vertical when at meridian). During the JKT run about 1000 spectra were obtained on about 200 stars.

Table 1. JKT observations: grating angle settings

night 1994	grating angle	wavelength range
March 28	24°	6000Å-8200Å
March 29	24°+27°	6000Å-8200Å+7600Å-9900Å
March 30	21°	4300Å-6500Å
March 31	18°	3200Å-5100Å
April 1	21°	4300Å-6500Å
April 2	24°	6000Å-8200Å
April 3	27°	7600Å-9900Å
April 4	18°	3200Å-5100Å

The spectrograph used at the Siding Spring 2.3m telescope was the Double Beam Spectrograph. This instrument has two beams split by a dichroic slide. The detectors were 2 1024×1024 CCD's, the blue channel CCD is UV coated. The grating used was also a 600 lines/mm giving a dispersion of 1.1Å/pixel (15 μm pixels). The slit width was 2 arcsec on the sky. The spectral resolution was less than 3 pixels FWHM with good focus, so about 3Å. The mode "vertical slit on sky" was used. Three configurations were defined:

- Configuration 1: wavelength range on blue channel: 3500-4500Å; on red channel: 6470-7550Å.
- Configuration 2: wavelength range on blue channel: 4475-5550Å; on red channel: 7500-8570Å.
- Configuration 3: wavelength range on blue channel: 5510-6550Å; on red channel: 8530-9650Å.

Table 2 summarizes the configurations used during this run. 36 stars were obtained at Siding Spring. They were selected mainly in the Large Magellanic Cloud or among local metal poor stars, in order to improve the coverage of stellar parameter space. Some Wolf Rayet stars were also observed.

3. Star selection

Most stars were originally selected from the catalogue of Cayrel de Strobel et al.(1992) according to the value of [Fe/H]. Additional samples of 62 and 45 stars were selected to include targets with either near-IR spectra (from Lançon & Rocca-Volmerange 1992) and/or UV data (from IUE) respectively.

The Tables 5 to 10 give the list of the 249 stars included in the library. Most of the atmospheric parameters (T_{eff}, log(g), [Fe/H]) listed in Tables 5 to 10 come from the 2

Table 2. SSO 2.3m spectrograph configurations (see text)

night 1994	config. number	wavelength ranges blue channel	red channel
December 25	1	3500Å-4500Å	6470Å-7550Å
December 26	2	4475Å-5550Å	7500Å-8570Å
December 27	3	5510Å-6550Å	8530Å-9650Å
December 28	1	3500Å-4500Å	6470Å-7550Å
December 29	2	4475Å-5550Å	7500Å-8570Å
December 30	3	5510Å-6550Å	8530Å-9650Å
December 31	1	3500Å-4500Å	6470Å-7550Å

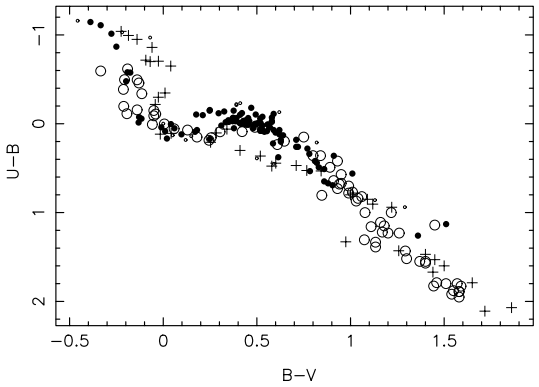

Fig. 1. U-B vs B-V for the stars in STELIB corrected for interstellar extinction. The different symbols represent different stellar spectral classes: full circles are dwarf main sequence stars (class V), open circles, giants (class III) and plus sign, super-giants of classes I and II. Small circles are used for stars with no spectral class determination.

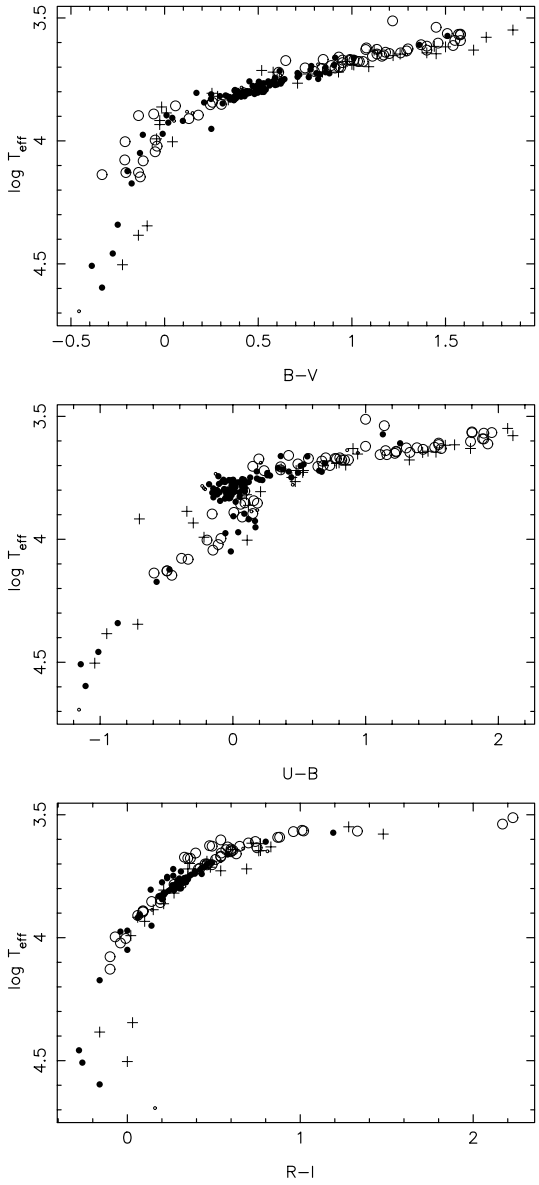

Fig. 2. T_{eff}vs B-V, U-B and R-I. The colors are corrected for interstellar extinction. Symbols are the same as in Fig. 1.

latest editions of the Catalogue of [Fe/H] determinations (Cayrel de Strobel et al. 1997, 2001). This compilation was complemented by accurate T_{eff} listed in Blackwell & Lynas-Gray (1998), di Benedetto (1998) and Alonso et al. (1996, 1999). We have also used the V-K colour index, when available, calibrated into T_{eff} using the formulae of Alonso et al. (1996, 1999). Multiple determinations of atmospheric parameters for the same star were averaged, giving more weight to the most recent ones. Several stars with unknown atmospheric parameters were also part of the ELODIE database (Prugniel & Soubiran 2001). In that case we give the parameters determined by the TGMET method (Katz et al. 1998).

Absolute magnitudes M_V were derived from the Hipparcos parallax and TYCHO2 V_T apparent magnitude, transformed into V Johnson band (Høg et al. 2000) and corrected with Av measured on the spectra. M_V is only given for stars having a relative parallax error lower than 30%. Uncertainties correspond to one σ errors on parallaxes and V magnitudes.

Most of the stars in the library have accurate UBV photometry available from the Lausanne "General Catalogue of Photometric Data" compiled by Mermilliod et al. (1997) and about half of them have R and I photometry. Fig. 1 shows the U-B vs B-V diagram corrected for the interstellar extinction with A_V/E_{B-V}=3.1, E_{U-V}/E_{B-V}=1.59, E_{R-V}/E_{B-V}=-0.88 and E_{I-V}/E_{B-V} = -1.60. The relations T_{eff} versus color indices are displayed in Fig. 2. Finally, HR-type diagrams are shown in Fig. 3. In the log(g)/T_{eff} diagram and M_V/T_{eff} diagrams, evolutionary tracks from the Geneva models (Schaller et al. 1992) are displayed for solar metallicity. In the diagram M_V versus T_{eff} and M_V versus B-V, M_V are from the Hipparcos catalog (Perryman et al., 1997). Fig. 4 shows the distribution of [Fe/H] as a function of T_{eff}.

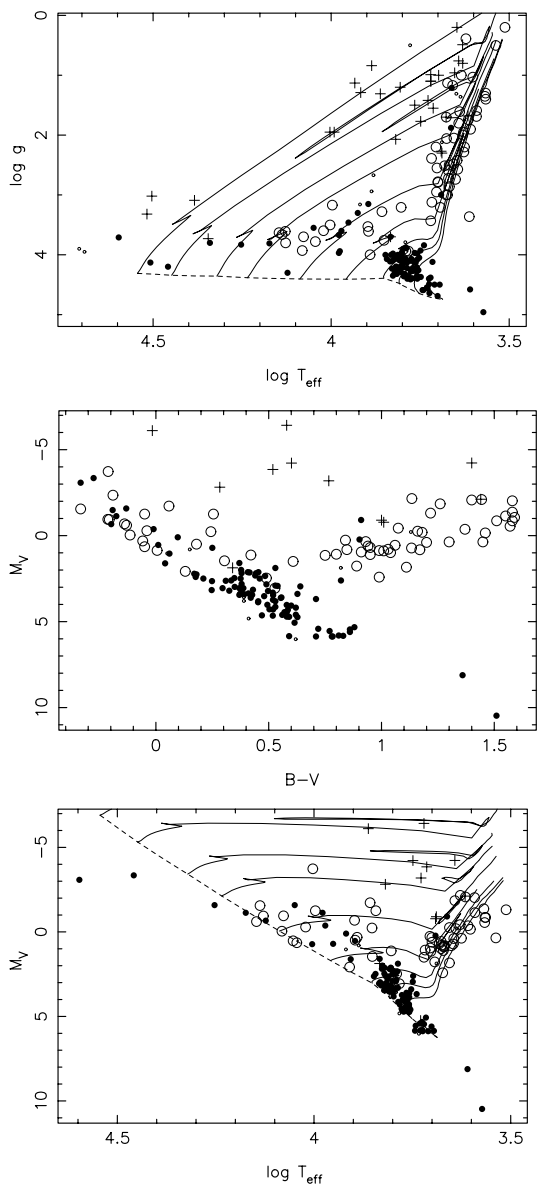

Fig. 3. Log(g) vs log(T_{eff}) and HR diagrams. Symbols are the same as in Fig. 1.

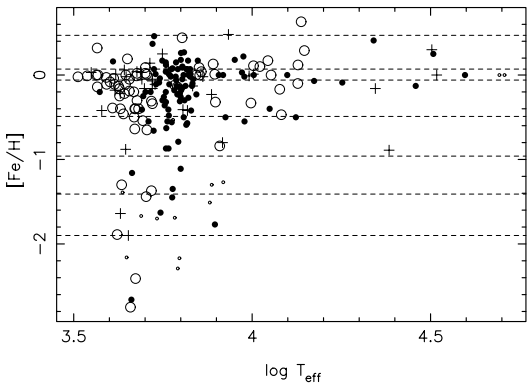

Fig. 4. Metallicity distribution. Symbols are the same as in Fig. 1. Horizontal lines show the limits of the subsets described in Table 11

Table 3. Standard stars observed at JKT

star	num. of spectra	rms	reference
HR2422	19	0.058	Whiteoak (1966)
HR3454, η Hya	31	0.024	Hamuy et al., 1992, 1994
HR4963, θ Vir	29	0.020	Hamuy et al., 1992, 1994, Hayes 1970
HR3982, Regulus	27	0.020	Cochran (1981), Hayes 1970
HR5511, 109 Vir	17	0.036	Cochran (1981), Johnson (1980)
HR7001, Vega	11	0.022	Hayes, 1985
HR7589	15	0.041	Whiteoak (1966)

4. Data reduction

The basic data reduction was performed with iraf[1] except for the flux calibration of JKT data which appeared to demand non-standard procedures.

The wavelength calibration was done thanks to the acquisition of arc spectra from a Cu-Ne lamp for the JKT data and from He-Ar, Ar-Ne and Cu-Ar lamps for the SSO data. The typical number of lines used was 30 to 50. The rms of the residuals is of the order of 0.1 Å.

Table 3 gives the list of the standard stars observed at JKT. In average, 18 spectra of standard stars were obtained each night, enough to allow checking for atmospheric extinction. The examination of these spectra revealed strongly varying atmospheric extinction during the observations. Our interpretation is that the strong wind blowing from east was carrying dust from the Sahara desert. But we cannot exclude that it comes from differential atmospheric loss in the JKT narrow slit.

As a consequence, the direct use of the standard stars spectra, with a standard procedure to flux calibrate the spectra was not feasible. We then built a procedure to take into account various factors which affect the atmospheric extinction both in its absolute value and its dependence with wavelength.

The normal atmospheric extinction is modeled by the mean atmospheric extinction curve versus wavelength and the airmass at time of observation. The "abnormal" extinction, possibly due to dust, is likely to change rapidly during one night. We calibrated this effect by using any observed star as a photometric standard star. The UBVRI photometry of most of our program stars are available in the Lausanne database (http://obswww.unige.ch/gcpd/gcpd.html) (Mermilliod et al., 1997). However to do this, it has been necessary to take the variation of seeing into account. The seeing, measured on each spectrum from the profile of the star

[1] IRAF is distributed by the National Optical Astronomy Observatories, USA, which are operated by the Association of Universities for Research in Astronomy, Inc., under cooperative agreement with the National Science Foundation, USA.

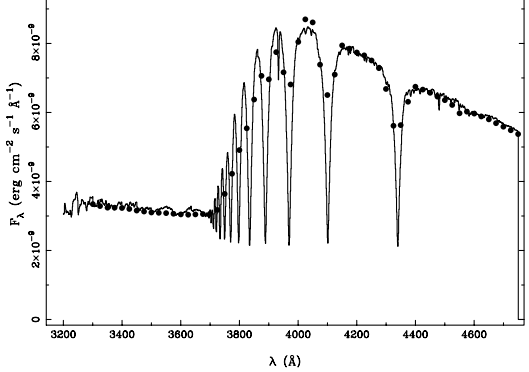

Fig. 5. Comparison of Vega spectrum in the UV with published SED (filled circles).

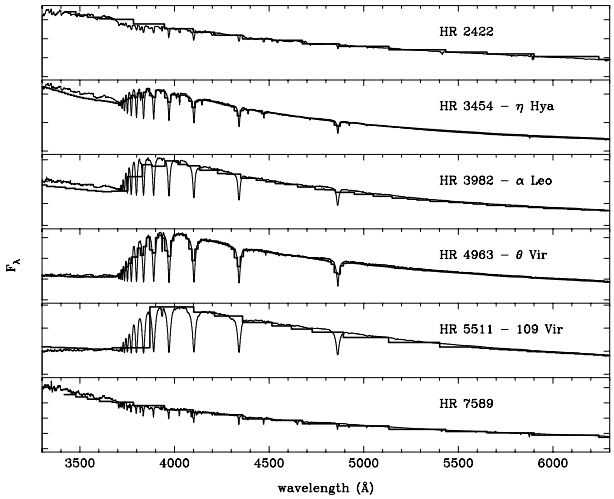

Fig. 6. Comparison of calibrated standard stars spectra observed at JKT with published SED (bold curve).

image along the slit, appeared to change significantly during the nights, typically between 0.6″and 1.5″. The light lost outside the slit differs as the seeing varies. To model it, we took into account the stellar profile and the slit width. The detailed modelling process was performed individually for each star. This operation gives an absolute mean value over the wavelength for a given grating angle setting to scale the spectra. Then, the observations of spectrophotometric standard stars were used to analyse the wavelength dependence of the additionnal extinction.

Fig. 5 and 6 show the comparison of the calibrated standard stars spectra with published SED. The spectrum of Vega (Fig. 5) was obtained only in the shortest wavelenth setting because of its brightness. The comparison for the other standards are shown in Fig. 6. The rms of difference between calibrated spectra of standard stars and published spectra, expressed in magnitude, are given in Table 3. They are computed avoiding the strong absorption lines where the difference of wavelength sampling introduces large dispersions.These rms are between 0.02 and 0.04 magnitude. An exception is HR2422 for which the rms is 0.058.

The SSO spectra were reduced using the standard procedures for flux calibration. Table 4 lists the standard stars used. Two target stars and one standard star observed in this run were also observed at JKT. We used these stars as an additional check on the reliability of the complex flux calibration procedure applied to JKT data. A good agreement was obtained between the two independent set of spectra. Fig. 7 shows the comparison of the calibrated standard stars spectra with published SED. As for the JKT standard stars, the rms of difference between calibrated spectra of standard stars and published spectra, are given in Table 4. They are also computed avoiding the strong absorption lines. The rms have similar values between 0.02 and 0.04 magnitude. One standard star, η Hya, has been observed during both runs. The rms of the difference is 0.031 magnitude, of the same order than the rms of the difference between observed and published spectra. Thus, we can consider that 0.03 magnitude is the typical absolute photometric uncertainty of the library. In addition, the detailed comparison between the synthetic photometry derived from the STELIB library and the Lausanne database is presented and discused in Appendix A. Tables A.3 to A.6 provide with the UVBRI synthetic photometry for STELIB stars.

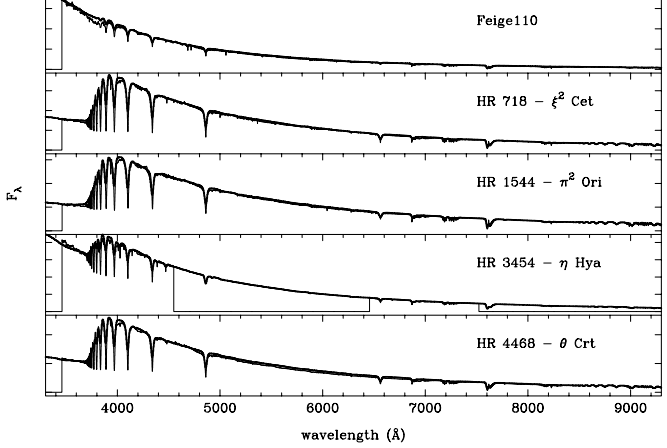

Fig. 7. Comparison of calibrated standard stars spectra observed at SSO 2.3m with published SED (bold curve).

Table 4. Standard stars observed at SSO

star	rms (mags)	reference
HR 3454, η Hya	0.024	Hamuy et al., 1992, 1994
HR 718, ξ^2 Cet	0.027	Hamuy et al., 1992, 1994
Feige 110	0.043	Oke,1990 , Hamuy et al., 1992, 1994
HR 4468, θ Crt	0.031	Hamuy et al., 1992, 1994
HR 1544, π^2 Ori	0.024	Hamuy et al., 1992, 1994

5. The library

Once calibrated, the spectra in the 4 (JKT) or 6 (SSO) settings of the program stars were combined by averaging

Star	RA 2000	DEC 2000	spectr.	Teff	log(g)	[Fe/H]	Mv	Av	identification
HD 2857	00:31:53.80	-05:15:42.3	A2	7611	2.67	-1.51		0.25	-
HD 5820	00:59:49.68	+06:28:59.6	M2III				$-2.10^{+0.53}_{-0.69}$	0.70	V* WW Psc
HD 6268	01:03:18.19	-27:52:49.7	G0III	4712	1.13	-2.41		0.60	-
HD 9138	01:30:10.94	+06:08:38.2	K4III	4061	1.90	-0.39	$-0.37^{+0.19}_{-0.20}$	0.00	μ Psc
HD 12479	02:02:35.08	+13:28:36.2	M2III				$-1.06^{+0.51}_{-0.66}$	0.00	-
HD 15318	02:28:09.52	+08:27:36.3	B9III	11300			$0.52^{+0.21}_{-0.23}$	0.08	ξ^2 Cet HR718
HD 18191	02:55:48.50	+18:19:54.0	M6IIIvar	3450	0.50	-0.01	$0.36^{+0.25}_{-0.27}$	0.00	ρ^2 Ari V* RZ Ari
HD 21581	03:28:54.45	-00:25:02.4	G0	4885	2.12	-1.67	$1.87^{+0.56}_{-0.74}$	0.00	-
HD 26630	04:14:53.86	+48:24:33.7	G0Ib	5345	1.42	-0.11	$-3.19^{+0.36}_{-0.42}$	0.6	μ. Per
HD 29574	04:38:55.74	-13:20:47.7	G8/K0IIIw.	4183	0.39	-1.89		1.0	V* HP Eri
HD 30739	04:50:36.72	+08:54:00.9	A1Vn				$0.37^{+0.18}_{-0.19}$	0.10	π^2 Ori HR 1544
HD 268623	04:52:11	-66:42:08	B2Ia					0.00	-
HD 268749	04:53:29	-69:24:34	B7Iab					0.00	-
HD 30614	04:54:03.01	+66:20:33.6	O9.5Iae	31888	3.02	0.30		0.79	α Cam
HD 32034	04:55:11	-67:10:10	B9Ia	8262	1.29	-0.80		0.39	-
HD 268819	04:55:32.46	-69:57:45.1	F6					0.00	-
HD 33133	05:03:08	-66:40:42	WN					0.00	LMC FD 12
HD 33579	05:05:55.51	-67:53:10.9	A3Ia	7694	0.84	-0.23		0.56	-
HD 32537	05:06:40.66	+51:35:53.3	F0V	6978	4.07	-0.23	$2.49^{+0.06}_{-0.06}$	0.4	12 Cam V* BM Cam
HD 32923	05:07:26.68	+18:38:42.0	G4V	5727	3.98	-0.20	$3.62^{+0.05}_{-0.05}$	0.3	104 Tau
HD 271163	05:18:52	-65:41:22	B3Ia					0.00	-
HD 34411	05:19:08.08	+40:06:02.4	G0V	5845	4.13	0.01	$4.19^{+0.04}_{-0.04}$	0.00	λ Aur
HD 34816	05:19:34.53	-13:10:36.4	B0.5IV	28724	4.20	-0.13	$-3.35^{+0.51}_{-0.65}$	0.02	λ Lep
HD 271182	05:21:01.71	-65:48:02.4	F8...	6000	0.50	-0.53		0.00	-
HD 35497	05:26:17.50	+28:36:28.3	B7III	13429	3.80	-0.10		0.03	β Tau
HD 269687	05:31:25	-69:05:35	B0e					0.00	-
HD 269697	05:31:38.42	-67:28:11.6	F5Ia					0.00	-
HD 269698	05:31:42	-67:38:06	O5e					0.00	-
HD 36512	05:31:55.86	-07:18:05.5	B0V	32200	4.13	0.25		0.4	υ Ori
HD 36673	05:32:43.81	-17:49:20.3	F0Ib	7276	1.31	-0.02	$-6.11^{+0.56}_{-0.74}$	0.7	α Lep
HD 37680	05:34:18	-69:45:00	WC					0.00	FD 46
HD 269781	05:34:22.47	-67:01:23.6	A0Iae					0.00	-
HD 38282	05:38:53	-69:02:01	WN					0.00	FD 70
HD 37828	05:40:54.62	-11:11:59.8	K0	4335	1.36	-1.39	$-0.21^{+0.44}_{-0.54}$	0.00	-
HD 37394	05:41:20.33	+53:28:56.4	K1V	5194	4.12	-0.20	$5.07^{+0.04}_{-0.04}$	0.7	-
HD 38247	05:45:11.52	+18:42:15.7	G8Iab	4755	1.70	0.04		2.0	-
HD 39587	05:54:23.08	+20:16:35.1	G0V	5915	4.39	-0.02	$4.72^{+0.04}_{-0.04}$	0.00	χ^1 Ori
HD 39801	05:55:10.29	+07:24:25.3	M2Ib	3540	0.00	0.03		0.00	α Ori V*
HD 39866	05:56:33.77	+28:56:32.2	A2II	10080	1.95	0.01		0.80	-
HD 39949	05:57:05.56	+27:19:00.1	G2Ib	5250	1.10	-0.16		0.5	-
HD 40111	05:57:59.66	+25:57:14.1	B1Ib					0.39	139 Tau
HD 41667	06:05:03.64	-32:59:39.3	G8V	4605	1.88	-1.16		0.00	-

Table 5. catalogue of the stars

the overlapping pixels. This results in 257 stellar spectra in *fits* format resampled with a step of 1Å per pixel. The library is available in two different forms: the "raw" data, including the combined spectra as coming out of the calibration process, and the data corrected for interstellar reddening using the empirical extinction function of Cardelli et al. (1989). As an additional check, we have compared the reddening corrected spectra (using the extintion values from the literature) to the equivalent ones in the Kurucz atlas (same spectral type and metallicity). In most cases (∼80%), the agreement between the two spectra is excellent. In case of discrepancy (∼20% of the sample), the extintion values used and quoted in the tables are those allowing to match our corrected spectra to Kurucz. These discrepant objects are clearly identifyed on the web site.

6. Synthetic spectra of stellar populations

Templates of stellar populations have been built from the dereddened library. At this stage, the wavelength scale was corrected for radial velocity. For some stars, data are missing in limited wavelength ranges: for these, we filled the gaps using spectra of stars of similar or close spectral type. The final spectra are useful from 3200 to 9300Å because spectra become noisy from 9300Å to 9850Å. In this

Star	RA 2000	DEC 2000	spectr.	Teff	log(g)	[Fe/H]	Mv	Av	identification
HD 41593	06:06:40.55	+15:32:32.5	K0V	5305	4.49	0.07	$5.81^{+0.05}_{-0.05}$	0.00	V* V1386 Ori
HD 41636	06:08:23.14	+41:03:21.0	G9III	4755	1.70	-0.30	$0.99^{+0.21}_{-0.23}$	0.00	-
HD 42454	06:12:05.49	+29:29:31.8	G2Ib	5250	1.10	-0.05		1.2	-
HD 42543	06:12:19.10	+22:54:30.7	M1Ia-ab	3789	0.00	-0.42		1.0	6 Gem V* BU Gem
HD 43153	06:15:25.13	+16:08:35.5	B7V	13263	4.30	-0.50	$-0.67^{+0.30}_{-0.34}$	0.15	72 Ori
HD 45829	06:30:02.29	+07:55:16.0	K0Iab	4435	0.20	-0.02		1.0	-
HD 46223	06:32:09.31	+04:49:24.7	O5e	49300	3.95			2.1	-
HD 47129	06:37:24.04	+06:08:07.4	O8V+...					1.13	HR2422
HD 47839	06:40:58.66	+09:53:44.7	O7Ve	39500	3.71		$-3.08^{+0.46}_{-0.58}$	0.26	15 Mon V* S Mon
HD 47731	06:41:20.90	+28:11:47.9	G5Ib	4990	1.00	-0.16		0.00	25 Gem
HD 48329	06:43:55.93	+25:07:52.2	G8Ib	4384	0.76	0.06	$-4.23^{+0.51}_{-0.65}$	0.00	ε Gem
HD 48682	06:46:44.34	+43:34:37.3	G0V	5727		0.15	$3.87^{+0.04}_{-0.04}$	0.3	ψ^5 Aur A
HD 48682B	06:46:46	+43:35:03	M0V					0.00	ψ^5 Aur B
HD 49933	06:50:49.82	-00:32:25.5	F2V	6538	4.32	-0.59	$3.20^{+0.07}_{-0.07}$	0.2	-
HD 50420	06:55:14.66	+43:54:36.2	A9III	7200	3.28	0.04	$-1.72^{+0.41}_{-0.50}$	0.75	V* V352 Aur
HD 52005	07:00:15.82	+16:04:44.4	K4Iab:	4271	0.80	-0.22		0.00	41 Gem
HD 52973	07:04:06.54	+20:34:13.1	G3Ibvar	5604	1.77	0.25	$-4.22^{+0.57}_{-0.76}$	0.4	ζ Gem V*
HD 53929	07:07:06.48	+04:54:38.2	B9.5III	14011	3.63	0.29	$-0.61^{+0.36}_{-0.42}$	0.00	-
HD 60778	07:36:11.79	-00:08:14.9	A1V	8416	3.30	-0.50		0.28	-
HD 61064	07:37:16.73	-04:06:39.7	F6III	6367	3.21	0.44	$1.12^{+0.13}_{-0.14}$	0.06	25 Mon
LHS 235	07:40:21	-17:24:54	DF					0.00	-
HD 63077	07:45:35.18	-34:10:35.6	G0V	5731	4.08	-0.87	$4.46^{+0.04}_{-0.04}$	0.00	171 Pup
HD 64090	07:53:32.64	+30:36:34.3	sdG2	5413	4.53	-1.70	$6.03^{+0.09}_{-0.09}$	0.00	-
HD 65583	08:00:32.24	+29:12:54.7	G8V	5295	4.64	-0.66	$5.87^{+0.05}_{-0.05}$	0.00	-
HD 67767	08:10:27.23	+25:30:29.4	G8IV	5598	4.37	0.17	$2.61^{+0.08}_{-0.09}$	0.00	ψ Cnc
HD 69897	08:20:03.87	+27:13:07.0	F6V	6275	4.21	-0.31	$3.82^{+0.05}_{-0.05}$	0.02	χ Cnc
HD 70272	08:22:50.13	+43:11:18.1	K5III	3900	1.59	-0.03	$-1.14^{+0.21}_{-0.23}$	0.00	31 Lyn V* BN Lyn
HD 72184	08:32:55.06	+38:01:00.4	K2III	4525	2.05	-0.05	$1.83^{+0.12}_{-0.13}$	0.00	-
HD 72324	08:33:00.14	+24:05:05.7	G9III	4743	2.06	-0.01	$0.79^{+0.29}_{-0.34}$	0.00	υ^2 Cnc
HD 74280	08:43:13.49	+03:23:55.2	B3V	17899	3.83	-0.09	$-1.59^{+0.29}_{-0.32}$	0.08	η Hya HR3454
HD 74739	08:46:41.83	+28:45:36.0	G8Iab:	4910	2.27	-0.05	$-0.78^{+0.27}_{-0.30}$	0.00	ι Cnc A
HD 75732	08:52:36.13	+28:19:53.0	G8V	5256	4.38	0.37	$5.46^{+0.04}_{-0.04}$	0.00	ρ Cnc A
HD 76151	08:54:18.19	-05:26:04.3	G3V	5728	4.40	0.04	$4.74^{+0.05}_{-0.05}$	0.1	-
HD 76943	09:00:38.75	+41:47:00.4	F5V	6575	4.03	0.07	$2.61^{+0.06}_{-0.06}$	0.3	10 UMa
HD 77350	09:02:44.27	+24:27:10.6	A0III	10506	3.60	0.10	$-0.29^{+0.29}_{-0.33}$	0.00	ν Cnc
HD 77729	09:05:04.74	+26:09:53.4	K4III	4271	2.00	-0.40		0.00	-
HD 78316	09:07:44.82	+10:40:05.6	B8IIImnp	13449	3.61	0.12	$-0.94^{+0.29}_{-0.33}$	0.3	kap Cnc V*
HD 78418	09:08:47.42	+26:37:48.0	G5IV	5659	4.05	-0.26	$3.39^{+0.08}_{-0.09}$	0.1	75 Cnc
HD 79158	09:13:48.23	+43:13:04.5	B8IIImnp	13727	3.66	0.63	$-1.55^{+0.31}_{-0.35}$	0.6	36 Lyn
HD 79452	09:15:14.36	+34:38:00.2	G6III	5072	2.20	-0.65	$0.26^{+0.28}_{-0.31}$	0.00	-
HD 80081	09:18:50.67	+36:48:10.4	A1V				$1.05^{+0.08}_{-0.08}$	0.00	38 Lyn
HD 81192	09:24:45.39	+19:47:12.8	G7III	4692	2.59	-0.64	$1.10^{+0.30}_{-0.34}$	0.00	-

Table 6. catalogue of the stars (cont'd)

way, we built several subsets of the atlas with different [Fe/H] ranges (Table 11). These subsets include a total of 242 star templates which are also available on the web site.

6.1. Comparison with Kurucz spectra

In order to compare with the previous results, and to show the capabilities of this new library, we have built galaxy models with the STELIB library in the apropriate subset, using the new galaxy evolutionary code GISSEL02 (Bruzual & Charlot 1993). The evolution of a single stel-

Table 11. Subsets of stars according to their metallicity

	[Fe/H] range	number of stars
	< -1.90	6
	[-1.90 , -1.41]	12
sub-solar	[-1.40 , -0.96]	6
	[-0.95 , -0.49]	23
	[-0.48 , -0.06]	69
solar	[-0.06 , +0.07]	84
above	[+0.08 , +0.47]	38
solar	> +0.47	4

Star	RA 2000	DEC 2000	spectr.	Teff	log(g)	[Fe/H]	Mv	Av	identification
HD 81809	09:27:46.92	-06:04:15.7	G2V	5610	3.93	-0.30	$2.95^{+0.09}_{-0.09}$	0.00	-
HD 82210	09:34:28.97	+69:49:48.6	G4III-IV	5253	3.43	-0.34	$1.50^{+0.06}_{-0.06}$	0.5	-
HD 83632	09:40:34.09	+26:00:14.4	K2III	4308	1.00	-1.30		0.3	-
HD 84937	09:48:55.87	+13:44:46.1	sdF5	6257	4.04	-2.17	$3.80^{+0.20}_{-0.22}$	0.00	-
HD 85235	09:52:06.36	+54:03:51.4	A3IV	11200	3.55	-0.40	$-1.58^{+0.24}_{-0.27}$	0.5	φ UMa
HD 86161	09:54:52.91	-57:43:38.3	WN					0.00	WR 16 V* V396 Car
HD 86728	10:01:01.02	+31:55:29.0	G1V	5737	4.25	0.12	$4.32^{+0.04}_{-0.04}$	0.2	20 LMi
HD 86986	10:02:29.48	+14:33:27.0	A1V	7867	3.15	-1.77	$0.54^{+0.51}_{-0.65}$	0.34	-
HD 87141	10:04:36.35	+53:53:30.2	F5V	6369	3.99	0.09	$2.14^{+0.09}_{-0.09}$	0.2	-
HD 87737	10:07:19.95	+16:45:45.6	A0Ib	9806	1.95	-0.01		0.04	η Leo
HD 87696	10:07:25.73	+35:14:40.9	A7V				$2.25^{+0.07}_{-0.07}$	0.00	21 LMi
HD 87822	10:08:15.94	+31:36:15.4	F4V	6615	4.07	0.17	$2.13^{+0.13}_{-0.13}$	0.1	-
HD 87901	10:08:22.46	+11:58:01.9	B7V	12540				0.08	α Leo Regulus HR3982
HD 88355	10:11:38.19	+13:21:18.7	F7V	6423		0.00	$2.19^{+0.14}_{-0.15}$	0.05	34 Leo
HD 88609	10:14:28.98	+53:33:39.6	G5IIIwe	4560	1.17	-2.75		0.00	-
HD 89025	10:16:41.40	+23:25:02.4	F0III	6965			$-1.25^{+0.15}_{-0.16}$	0.17	ζ Leo
HD 89254	10:17:37.90	-08:04:08.1	F2III	7106	3.76	0.09	$1.46^{+0.11}_{-0.11}$	0.05	ε Sex
HD 89758	10:22:19.80	+41:29:58.0	M0III	3700	1.35	0.00	$-1.37^{+0.14}_{-0.14}$	0.00	μ UMa
HD 90277	10:25:54.87	+33:47:46.5	F0V	8937	3.46	0.18	$0.71^{+0.12}_{-0.13}$	0.00	30 LMi
HD 90508	10:28:03.81	+48:47:13.4	G1V	5735	4.35	-0.32	$4.28^{+0.06}_{-0.06}$	0.3	-
HD 90537	10:27:53.09	+36:42:26.9	G8III-IV	5061	2.95	0.01	$0.95^{+0.10}_{-0.10}$	0.00	β LMi
HD 90839	10:30:37.76	+55:58:50.2	F8V	6052	4.36	-0.18	$4.29^{+0.04}_{-0.04}$	0.00	36 UMa
HD 91316	10:32:48.68	+09:18:23.7	B1Ib	24200	3.09	-0.89		0.0	ρ Leo V*
HD 92740	10:41:17.52	-59:40:36.9	WNs...					1.30	WR 22 V* V429 Car
HD 92809	10:41:38.33	-58:46:18.8	WC					0.00	WR 23
HD 92769	10:43:01.95	+26:19:32.5	A4Vn	6380	4.10	-0.15	$2.22^{+0.09}_{-0.10}$	0.00	40 LMi
HD 93250	10:44:45.04	-59:33:54.7	O5	51000	3.90			1.58	-
HD 93430	10:47:22.18	+16:55:20.7	G0				$3.90^{+0.30}_{-0.34}$	0.00	-
HD 93765	10:49:53.73	+27:58:25.9	F5V	6811	3.70	-0.10	$1.59^{+0.14}_{-0.15}$	0.00	44 LMi
HD 94028	10:51:28.29	+20:16:43.0	F4V	5969	4.28	-1.45	$4.63^{+0.15}_{-0.16}$	0.0	-
HD 94264	10:53:18.64	+34:12:56.0	K0III-IV	4657	2.86	-0.20	$0.81^{+0.07}_{-0.07}$	0.6	46 LMi
HD 94247	10:53:34.52	+54:35:06.5	K3III	4243	2.28	-0.16	$-2.16^{+0.28}_{-0.32}$	0.7	44 UMa
HD 95345	11:00:33.64	+03:37:03.1	K1III	4527	2.48	-0.19	$-0.26^{+0.22}_{-0.24}$	0.00	58 Leo
HD 95418	11:01:50.39	+56:22:56.4	A1V	9452	3.94	0.22		0.3	β UMa
HD 95735	11:03:20.61	+35:58:53.3	M2V	3739	4.96	-0.20	$10.47^{+0.03}_{-0.03}$	0.00	-
HD 97633	11:14:14.44	+15:25:47.1	A2V	9360	3.60	0.03	$-0.38^{+0.11}_{-0.11}$	0.00	θ Leo
HD 97916	11:15:54.11	+02:05:12.2	F5V	6308	4.08	-1.11	$3.61^{+0.36}_{-0.41}$	0.00	-
HD 98262	11:18:28.76	+33:05:39.3	K3III	4119	1.74	-0.11	$-2.07^{+0.23}_{-0.25}$	0.00	ν UMa
HD 98839	11:22:49.61	+43:28:57.9	G8II	4886	2.30	0.03	$-0.90^{+0.21}_{-0.23}$	0.00	56 UMa
HD 99028	11:23:55.37	+10:31:46.9	F2IV	6703	3.98	0.07	$1.99^{+0.08}_{-0.08}$	0.1	ι Leo
HD 99747	11:29:04.70	+61:46:40.0	F5Vawvar	6580	4.23	-0.57	$3.05^{+0.06}_{-0.06}$	0.2	-
HD 100006	11:30:29.08	+18:24:35.1	K0III	4755	3.00	0.02	$0.56^{+0.20}_{-0.22}$	0.00	86 Leo

Table 7. catalogue of the stars (cont'd)

lar population of solar metallicity (Z=0.02) is given in Fig. 8 and 9, for ages of the stellar population ranging from 1 to 12 Gyr. A comparison with the same models obtained with the synthetic stellar spectra from Kurucz is also shown to emphasize the gain in spectral resolution.

6.2. Modeling observed spectra of galaxies

An important application of STELIB is to reproduce in details the spectral features observed in galaxies at $z \lesssim 1$. As an example, we present here the modeling of spectra of galaxies belonging to the cluster AC114 (more officially named ACO S 1077, Abell et al., 1989) at a redshift of z=0.312, and some foreground galaxies in the same field. These spectra were obtained with the spectrograph FORS1 on VLT unit 1 Antu, on october 5, 1999. The main objective of the run was the determination of the redshift of background lensed galaxies, but spectra of cluster galaxies were also obtained in the remaining slits. The grism used was G300V, with a wavelength coverage between ∼4000Å and ∼8600Å, and a wavelength resolution of R=500 for the 1" slit width used which correspond to a resolution of ∼7Å at rest frame of the cluster. Details

Star	RA 2000	DEC 2000	spectr.	Teff	log(g)	[Fe/H]	Mv	Av	identification
HD 100889	11:36:40.95	-09:48:08.1	B9.5Vn				$-0.20^{+0.17}_{-0.18}$	0.01	θ Crt HR4468
HD 101501	11:41:03.03	+34:12:09.2	G8Vvar	5380	4.55	-0.11	$5.42^{+0.03}_{-0.03}$	0.00	61 UMa
HD 101606	11:41:34.50	+31:44:45.5	F4V	6210	4.32	-0.79	$2.49^{+0.08}_{-0.08}$	0.2	62 UMa
LTT4364	11:45:43	-64:50:29	DC:					0.00	-
HD 102212	11:45:51.57	+06:31:47.3	M0III	3660			$-0.86^{+0.17}_{-0.18}$	0.00	ν Vir
HD 102224	11:46:03.13	+47:46:45.6	K0III	4358	1.61	-0.46	$-0.20^{+0.09}_{-0.10}$	0.00	χ UMa
HD 102634	11:49:01.40	-00:19:07.2	F7V	6314	4.12	0.18	$3.47^{+0.09}_{-0.09}$	0.00	-
HD 102870	11:50:41.29	+01:45:55.4	F8V	6121	4.13	0.15	$3.31^{+0.04}_{-0.04}$	0.10	β Vir
HD 103036	11:51:50.13	-05:45:43.8	G3Ibpvar	4275	0.49	-1.64		0.5	V* TY Vir
HD 104893	12:04:43.15	-29:11:05.1	K0I	4500	0.96	-1.90		0.00	-
HD 105546	12:09:02.76	+59:01:05.7	G2IIIw	5224	2.39	-1.37		0.6	-
HD 106038	12:12:01.50	+13:15:44.5	F6V-VI	5988	4.41	-1.35	$4.55^{+0.38}_{-0.44}$	0.4	-
HD 107213	12:19:29.66	+28:09:26.0	F8Vs	6318	4.06	0.26	$2.90^{+0.10}_{-0.10}$	0.00	9 Com
HD 108177	12:25:34.98	+01:17:06.4	sdF5	6069	4.33	-1.69	$4.82^{+0.28}_{-0.32}$	0.06	-
HD 109995	12:38:47.69	+39:18:32.9	A0p	8293	3.16	-1.27	$1.04^{+0.38}_{-0.45}$	0.0	-
HD 110897	12:44:59.68	+39:16:42.9	G0V	5845	4.24	-0.48	$4.66^{+0.04}_{-0.04}$	0.1	10 CVn
HD 111028	12:46:22.38	+09:32:26.8	K1III-IV	4710	3.00	-0.40	$2.41^{+0.11}_{-0.12}$	0.00	33 Vir
HD 112300	12:55:36.48	+03:23:51.4	M3III	3684	1.30	-0.14	$-0.55^{+0.13}_{-0.14}$	0.00	δ Vir
HD 113022	13:00:38.86	+18:22:22.3	F6Vs	6380	4.20	0.10	$3.15^{+0.09}_{-0.09}$	0.00	-
HD 113139	13:00:43.59	+56:21:58.8	F2V				$2.40^{+0.05}_{-0.05}$	0.6	78 UMa
HD 113337	13:01:47.15	+63:36:36.6	F6V	6545	4.20	0.07	$3.05^{+0.06}_{-0.06}$	0.1	-
HD 113226	13:02:10.76	+10:57:32.8	G8IIIvar	5017	2.79	0.09	$0.34^{+0.08}_{-0.08}$	0.00	ε Vir
HD 113848	13:06:21.28	+21:09:12.6	F4V	6628	4.03	-0.27	$2.47^{+0.16}_{-0.17}$	0.1	39 Com
HD 114330	13:09:57.01	-05:32:20.1	A1V	9509	3.67	-0.02	$-1.13^{+0.30}_{-0.35}$	0.00	θ Vir HR4963
HD 115383	13:16:46.71	+09:25:25.3	G0Vs	5981	4.10	0.08	$3.73^{+0.05}_{-0.05}$	0.19	59 Vir
HD 116842	13:25:13.42	+54:59:16.8	A5V	8066			$1.61^{+0.05}_{-0.05}$	0.4	80 UMa ALCOR
HD 117176	13:28:25.95	+13:46:48.7	G5V	5485	3.84	-0.09	$3.68^{+0.05}_{-0.05}$	0.00	70 Vir
HD 120136	13:47:16.04	+17:27:24.4	F7V	6445	4.22	0.27	$3.52^{+0.04}_{-0.04}$	0.00	τ Boo
HD 122408	14:01:38.78	+01:32:40.5	A3V	8290			$0.10^{+0.14}_{-0.15}$	0.01	τ Vir
HD 122563	14:02:31.96	+09:41:10.6	F8IV	4588	1.21	-2.66	$-0.91^{+0.40}_{-0.48}$	0.00	-
HD 123299	14:04:23.43	+64:22:32.9	A0III	9927	3.17	-0.33	$-1.25^{+0.12}_{-0.13}$	0.00	α Dra
HD 124425	14:13:40.67	-00:50:42.4	F7Vw	6380	4.04	0.09	$2.12^{+0.11}_{-0.12}$	0.05	-
HD 124570	14:14:05.33	+12:57:34.5	F6IV	6192	4.06	0.07	$2.93^{+0.07}_{-0.07}$	0.00	14 Boo
HD 124850	14:16:00.88	-05:59:58.3	F7V	6143	3.89	-0.13	$2.34^{+0.06}_{-0.06}$	0.08	ι Vir
HD 125560	14:19:45.32	+16:18:24.5	K3III	4426	2.42	0.00	$0.72^{+0.10}_{-0.11}$	0.3	20 Boo
HD 126141	14:23:06.92	+25:20:16.9	F5V	6632	4.30	0.00	$3.45^{+0.08}_{-0.08}$	0.00	-
HD 126660	14:25:12.02	+51:51:06.2	F7V	6369	4.29	-0.05	$3.22^{+0.03}_{-0.03}$	0.01	θ Boo
HD 127665	14:31:49.86	+30:22:16.1	K3III	4251	1.95	-0.25	$-0.43^{+0.10}_{-0.10}$	0.7	ρ Boo
HD 128167	14:34:40.69	+29:44:41.3	F3Vwva	6746	4.23	-0.42	$3.17^{+0.04}_{-0.04}$	0.35	σ Boo
HD 130109	14:46:14.99	+01:53:34.6	A0V	10110			$0.72^{+0.09}_{-0.09}$	0.02	109 Vir HR5511
HD 130948	14:50:15.72	+23:54:42.4	G2V	5947	4.07	0.07	$4.61^{+0.05}_{-0.05}$	0.00	-
HD 131156	14:51:23.28	+19:06:02.3	G8V	5512	4.59	-0.04	$5.55^{+0.03}_{-0.03}$	0.00	ξ Boo

Table 8. catalogue of the stars (cont'd)

of the observation conditions and data reduction can be found in Campusano et al. (2001).

A simple best fit procedure has been used to determine the spectral type of each galaxy, acording to its spectral features (see table 12). We have chosen to display galaxies of different types, from E to irregulars, with good S/N ratio. The models correspond to the evolution with time of a Single Stellar Population (SSP) built with the STELIB library for solar metallicity, assuming Kroupa (2001) IMF. The comparison between observed and modeled spectra is shown in Fig. 10. The best model was chosen among SEDs computed at 11 different ages from 100 Myr to 12 Gyr. The gain in spectral resolution is clear, with obvious applications in stellar population synthesis modelling. In particular, STELIB allows to determine the stellar populations using the strengths of a large number of absorption lines, due to the wide spectral coverage, and thus to improve the emission-line measurements in star-forming galaxies and AGNs.

7. Conclusions

We have presented the main characteristics of the public stellar library STELIB, available on the web site

Star	RA 2000	DEC 2000	spectr.	Teff	log(g)	[Fe/H]	Mv	Av	identification
HD 132142	14:55:12.00	+53:40:45.1	K1V	5125	4.50	-0.55	$5.87^{+0.05}_{-0.05}$	0.00	-
HD 134083	15:07:17.95	+24:52:10.5	F5V	6583	4.20	0.06	$3.45^{+0.05}_{-0.05}$	0.01	45 Boo
HD 134169	15:08:18.06	+03:55:50.3	G1Vw	5827	3.97	-0.87	$3.82^{+0.17}_{-0.18}$	0.00	-
HD 135722	15:15:30.10	+33:18:54.4	G8III	4803	2.51	-0.40	$0.69^{+0.06}_{-0.06}$	0.00	δ Boo
HD 136202	15:19:18.58	+01:46:00.0	F8III-IV	6068	3.94	-0.12	$3.06^{+0.06}_{-0.06}$	0.04	5 Ser V* MQ Ser
HD 136512	15:20:08.64	+29:36:58.7	K0III	4686	2.72	-0.40	$0.89^{+0.15}_{-0.16}$	0.00	o CrB
HD 137759	15:24:55.78	+58:57:57.7	K2III	4472	2.74	0.19	$0.82^{+0.05}_{-0.05}$	0.00	ι Dra
HD 138290	15:30:55.42	+08:34:44.8	F4Vw	6834	4.11	-0.05	$3.05^{+0.12}_{-0.12}$	0.00	-
HD 139669	15:31:25.05	+77:20:57.6	K5III	3907	1.69	-0.11	$-2.03^{+0.28}_{-0.31}$	0.00	θ UMi
HD 139641	15:37:49.55	+40:21:11.8	G8III-IV	4937	3.21	-0.54	$1.77^{+0.08}_{-0.08}$	0.00	φ Boo
HD 139798	15:38:16.14	+46:47:52.8	F2V	6788	4.00	-0.13	$2.98^{+0.06}_{-0.06}$	0.00	-
HD 141004	15:46:26.75	+07:21:11.7	G0Vvar	5899	4.22	-0.01	$4.07^{+0.04}_{-0.04}$	0.00	λ Ser
HD 141714	15:49:35.70	+26:04:06.8	G5III-IV	5218	3.12	-0.31	$1.08^{+0.10}_{-0.10}$	0.00	δ CrB
HD 142373	15:52:40.19	+42:27:00.0	F9V	5823	4.11	-0.41	$3.60^{+0.04}_{-0.04}$	0.01	χ Her
HD 144206	16:02:47.85	+46:02:12.7	B9III	11957	3.70	-0.17	$-0.95^{+0.16}_{-0.16}$	0.35	υ Her
HD 145675	16:10:24.21	+43:49:06.1	K0V	5312	4.40	0.46	$5.32^{+0.04}_{-0.04}$	0.00	14 Her
HD 145976	16:12:45.43	+26:40:14.4	F3V	6720	4.10	0.01	$2.18^{+0.14}_{-0.15}$	0.00	-
HD 146051	16:14:20.77	-03:41:38.3	M1III	3679	1.40	0.32	$-0.86^{+0.13}_{-0.14}$	0.00	δ Oph
HD 147394	16:19:44.45	+46:18:47.8	B5IV	14908	3.81	-0.07	$-1.13^{+0.13}_{-0.13}$	0.08	τ Her
HD 147547	16:21:55.24	+19:09:10.9	A9III	7125			$-0.23^{+0.11}_{-0.11}$	0.08	V* γ Her
HD 148513	16:28:33.98	+00:39:54.6	K4IIIp	4003	1.03	-0.08	$-0.16^{+0.25}_{-0.28}$	0.00	-
HD 148783	16:28:38.52	+41:52:54.1	M6IIIvar	3250	0.20	-0.02	$-1.31^{+0.16}_{-0.17}$	1.0	V* g Her 30 Her
HD 150275	16:30:39.08	+77:26:45.1	K1III	4667	2.50	-0.50	$0.87^{+0.17}_{-0.18}$	0.00	-
HD 149121	16:32:35.68	+05:31:16.4	B9.5III	11067	3.78	0.17	$0.64^{+0.21}_{-0.23}$	0.00	28 Her
HD 149661	16:36:21.18	-02:19:25.8	K2V	5362	4.56	0.01	$5.82^{+0.04}_{-0.04}$	0.00	12 Oph V* V2133 Oph
HD 151044	16:42:27.69	+49:56:12.1	F8V	6110	4.40	-0.02	$4.14^{+0.05}_{-0.05}$	0.00	-
HD 151217	16:45:49.89	+08:34:57.3	K5III	4093	3.36	-0.04	$0.00^{+0.21}_{-0.22}$	0.00	43 Her
HD 152830	16:55:15.97	+13:37:12.0	F5II	6811	3.70	-0.13	$1.87^{+0.15}_{-0.15}$	0.00	V* V644 Her
HD 154417	17:05:16.83	+00:42:12.1	F9V	5859	4.27	-0.11	$4.45^{+0.06}_{-0.06}$	0.00	V* V2213 Oph
HD 154733	17:06:18.11	+22:05:03.3	K4III	4220	2.20	-0.13	$0.37^{+0.19}_{-0.20}$	0.00	-
HD 155646	17:12:54.33	+00:21:07.9	F6III	6168	3.94	-0.14	$2.47^{+0.16}_{-0.17}$	0.00	-
HD 156283	17:15:02.85	+36:48:33.0	K3IIvar	4128	1.68	-0.18	$-2.12^{+0.14}_{-0.15}$	0.00	π Her
HD 157373	17:20:33.60	+48:11:19.7	F6Vawvar	6433	4.09	-0.50	$3.36^{+0.08}_{-0.08}$	0.00	-
HD 157214	17:20:39.47	+32:28:13.0	G0V	5686	4.26	-0.36	$4.60^{+0.03}_{-0.03}$	0.00	72 Her
HD 157089	17:21:07.15	+01:26:32.6	F9V	5786	4.13	-0.55	$4.03^{+0.10}_{-0.10}$	0.00	-
HD 157856	17:25:57.84	-01:39:06.9	F3V	6327	3.96	-0.18	$2.50^{+0.12}_{-0.13}$	0.00	-
HD 157881	17:25:45.57	+02:06:51.5	K7V	4073	4.58	0.16	$8.12^{+0.04}_{-0.04}$	0.00	-
HD 157999	17:26:30.88	+04:08:25.2	K3IIvar	4146		0.01		0.00	σ Oph
HD 159181	17:30:25.98	+52:18:04.9	G2II	5169	1.55	0.14	$-3.85^{+0.13}_{-0.14}$	1.4	β Dra
HD 159332	17:33:22.84	+19:15:24.8	F6V	6172	3.88	-0.23	$2.83^{+0.07}_{-0.08}$	0.00	-
HD 160693	17:39:37.24	+37:11:08.7	G0V	5747	4.21	-0.63	$4.71^{+0.11}_{-0.12}$	0.00	-
HD 160910	17:41:58.64	+15:57:07.8	F4Vw	6502	4.00	-0.13	$2.81^{+0.08}_{-0.08}$	0.00	-

Table 9. catalogue of the stars (cont'd)

http://webast.ast.obs-mip.fr/stelib. The main improvements with respect to other previous libraries are:

1. The homogeneous and relatively large spectral coverage, from 3200 to 9500Å.
2. The high spectral resolution and sampling for such a spectral coverage.
3. The wide metallicity range, although the present sample still needs some completion for extreme metallicities.

We have presented some qualitative examples on the possible use of STELIB for population synthesis and evolutionary models of galaxies. Fundamental Plane studies of high redshift galaxies could be another possible application for STELIB (Treu et al. 2001). In general, STELIB should be a useful tool for detailed studies of galaxies at $z \lesssim 1$, based on optical spectra at intermediate resolution.

Acknowledgements. We would like to thanks J.-C. Mermilliod who provided us a file extracted from the Lausanne photometric database. Many thanks to Stépane Charlot for a careful reading of the manuscript. This research has made use of the SIMBAD database, operated at CDS, Strasbourg, France. We are grateful to the help of the staff of Roque de los Muchachos Observatory at La Palma and of Siding Spring Observatory in Australia, where these observations were conducted. Some examples shown in this paper come from obser-

Star	RA 2000	DEC 2000	spectr.	Teff	log(g)	[Fe/H]	Mv	Av	identification
HD 161817	17:46:40.65	+25:44:57.3	sdA2	7702	2.94	-1.30	$0.80^{+0.25}_{-0.28}$	0.0	-
HD 163506	17:55:25.19	+26:02:59.9	F2Iavar	6400	1.20	-0.41		0.27	89 Her V* V441 Her
HD 163993	17:57:45.83	+29:14:52.5	K0III	5014	2.78	0.02	$0.61^{+0.06}_{-0.06}$	0.00	ξ Her
HD 164136	17:58:30.15	+30:11:21.4	F2II	6586	2.07	-0.42	$-2.82^{+0.29}_{-0.33}$	0.30	ν. Her V*
HD 164349	18:00:03.42	+16:45:03.4	K0II-III	4383	1.80	-0.22	$-1.85^{+0.35}_{-0.41}$	0.00	93 Her
HD 164353	18:00:38.72	+02:55:53.7	B5Ib	22150	3.73	-0.16		0.35	67 Oph
HD 165195	18:04:40.09	+03:46:45.4	K3p	4450	1.31	-2.16		0.00	-
HD 165341	18:05:27.21	+02:30:08.8	K0V	5025	4.69	-0.20	$5.60^{+0.03}_{-0.03}$	0.00	70 Oph V* V2391 Oph
HD 165908	18:07:01.61	+30:33:42.7	F7V	5952	4.26	-0.56	$4.02^{+0.04}_{-0.04}$	0.08	99 Her
HD 166620	18:09:37.65	+38:27:32.1	K2V	4955	4.50	-0.25	$5.86^{+0.03}_{-0.03}$	0.3	-
HD 166285	18:09:54.01	+03:07:13.1	F5V	6271	3.90	-0.22	$2.32^{+0.09}_{-0.09}$	0.00	-
HD 168151	18:13:53.36	+64:23:49.9	F5V	6463	4.05	-0.30	$2.64^{+0.04}_{-0.04}$	0.5	36 Dra
HD 167858	18:17:04.85	+01:00:20.9	F2V	7041	4.00	0.17	$2.63^{+0.13}_{-0.13}$	0.00	-
HD 172167	18:36:56.19	+38:46:58.8	A0Vvar	9520	3.97	-0.55		0.01	α Lyr Vega HR7001
HD 173780	18:46:04.47	+26:39:43.5	K3III	4413	2.57	-0.11	$0.39^{+0.11}_{-0.11}$	0.00	-
HD 173880	18:47:01.22	+18:10:52.4	A5III	8113		-0.84	$2.07^{+0.06}_{-0.06}$	0.0	111 Her
HD 175305	18:47:05.73	+74:43:30.8	G5III	5046	2.55	-1.44	$1.15^{+0.21}_{-0.23}$	0.00	-
HD 173819	18:47:28.98	-05:42:18.3	K0Ibpvar	4421	0.00	-0.88		0.00	V* R Sct
HD 175640	18:56:22.66	-01:47:59.3	B9III	12067	3.93	-0.47	$-0.04^{+0.26}_{-0.29}$	0.2	-
HD 176437	18:58:56.62	+32:41:22.4	B9III	10080	3.50	0.11	$-3.73^{+0.22}_{-0.24}$	0.5	γ Lyr
HD 176303	18:59:05.73	+13:37:21.2	F8V	6122	4.22	-0.06	$1.88^{+0.09}_{-0.09}$	0.00	11 Aql
HD 181470	19:19:01.15	+37:26:43.1	A0III	7887	3.53	-0.32	$-0.69^{+0.25}_{-0.27}$	0.4	-
HD 182101	19:22:48.35	+09:54:46.4	F6V	6303	4.18	-0.26	$3.41^{+0.09}_{-0.09}$	0.18	-
HD 182490	19:24:22.08	+16:56:15.9	A2III-IV				$0.86^{+0.23}_{-0.26}$	0.2	2 Sge
HD 338529	19:32:31.91	+26:23:27.6	B5	6192	3.79	-2.29	$3.58^{+0.45}_{-0.55}$	0.00	-
HD 184960	19:34:19.76	+51:14:13.5	F7V	6249	4.36	-0.14	$3.38^{+0.04}_{-0.04}$	0.3	-
HD 184927	19:35:32.01	+31:16:35.9	B2V	21913	3.80	0.41		0.25	V* V1671 Cyg
HD 185395	19:36:26.54	+50:13:13.7	F4V	6704	4.35	-0.02	$3.15^{+0.04}_{-0.04}$	0.00	θ Cyg
HD 185657	19:37:56.68	+49:17:02.6	G6V	4912	3.00	-0.41	$0.22^{+0.20}_{-0.22}$	0.30	-
HD 188209	19:51:59.07	+47:01:38.5	O9.5Ia	32903	3.32			0.70	HR7589
HD 187929	19:52:28.36	+01:00:20.4	F6Ib:	5826	1.50	0.07		0.00	η Aql V*
HD 188665	19:53:17.37	+57:31:24.5	B5V				$-1.49^{+0.22}_{-0.24}$	0.16	23 Cyg
HD 188510	19:55:09.70	+10:44:24.9	G5Vwe	5536	4.59	-1.63	$5.85^{+0.13}_{-0.13}$	0.00	2.52
HD 189849	20:01:06.01	+27:45:12.8	A4III	7860	3.61	0.01	$0.49^{+0.11}_{-0.11}$	0.00	15 Vul V* NT Vul
HD 194093	20:22:13.70	+40:15:24.1	F8Ib	5253	0.99	-0.07	$-6.42^{+0.48}_{-0.61}$	0.28	γ Cyg
HD 195725	20:29:34.83	+62:59:38.9	A7III	7769	4.00	0.13	$0.31^{+0.06}_{-0.07}$	0.8	θ Cep
HD 195986	20:32:52.33	+43:11:29.7	B4III				$-2.36^{+0.57}_{-0.76}$	0.25	-
HD 197345	20:41:25.91	+45:16:49.2	A2Ia	8582	1.13	0.48		0.36	α Cyg Deneb HD 197345
Feige110	23:19:58.40	-05:09:56.2	DA:					0.00	-

Table 10. catalogue of the stars (cont'd)

vations collected at the European Southern Observatory, Chile (ESO N 64.O-0439). Part of this work was supported by the French *Centre National de la Recherche Scientifique*, and by the French *Programme National Galaxies* (PNG). G. Bruzual acknowledges ample support from the Venezuelan Ministerio de Ciencia y Tecnología and FONACIT. G. Bruzual also thanks Observatoire Midi-Pyrénées and the MENRT for their support during stays in Toulouse.

References

Abell, G. O., Corwin, H. G. Jr, & Olowin, R. P. 1989, ApJS 70, 1.

Alonso, A., Arribas, S., & Martínez-Roger, C. 1996, A&AS 117, 227

Alonso, A., Arribas, S., & Martínez-Roger, C. 1999, A&AS 140, 261

Blackwell, D. E. & Lynas-Gray, A. E. 1998, A&AS 129, 505

Boisson, C., Joly, M., Moultaka, J., Pelat, D., Serote Roos, M. 2000, A&A 357, 850

Bruzual, G., & Charlot, S. 20033, submitted

Buzzoni, A. 1989, ApJS, 71, 817

Campusano, L. E., Pello, R., Kneib, J.-P., Le Borgne, J.-F., et al., 2001, A&A, 378, 394

Cardelli, J. A., Clayton, G. C., & Mathis, J. S. 1989, ApJ 345, 245

Cochran, A. L. 1981, ApJS 45, 83

Cayrel de Strobel, G., Hauck, B., Francois, P., et al. 1992, A&AS 95, 273

Cayrel de Strobel, G., Soubiran, C., Friel, E. D., Ralite, N., & Francois, P. 1997, A&AS 124, 299

Cayrel de Strobel, G., Soubiran, C. & Ralite, N. 2001, A&A 373, 159

Table 12. list of modeled galaxy spectra in the field of AC114

USNO	ident.in fig. 10	ra(2000)	dec(2000)	exposure time	redshift	spectral type	age of model
U0525_44063178	a	22:59:00.61	-34:46:20.8	2700s	0.1418	elliptical	12 Gyr
	b	22:58:37.19	-34:49:27.8	5400s	0.2605	irregular	500 Myr
U0525_44063148	c	22:58:43.07	-34:48:48.1	5400s	0.2999	irregular	500 Myr
	d	22:58:56.93	-34:47:57.4	2700s	0.3113	spiral	1 Gyr
	e	22:58:46.51	-34:49:09.6	4218s	0.3139	elliptical	12 Gyr
U0525_44062505	f	22:58:37.67	-34:49:24.8	4218s	0.3147	elliptical	12 Gyr
U0525_44063303	g	22:58:44.48	-34:49:11.3	4218s	0.3163	elliptical	12 Gyr
U0525_44063178	h	22:58:43.35	-34:49:36.5	5400s	0.3207	irregular	500 Myr

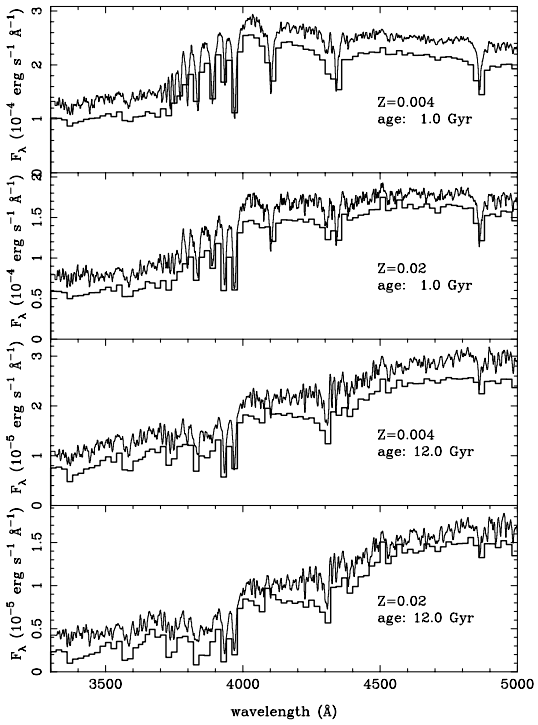

Fig. 8. Synthetic spectra built with STELIB compared to synthetic spectra obtained with Kurucz spectra using GISSEL02. SSP, wavelength range 3300Å to 5000Å, Z=0.02 (solar metallicity) and Z=0.004, from 1 Gyr to 12 Gyr. The Kurucz spectra are shifted downward by 10% of the scale for clarity.

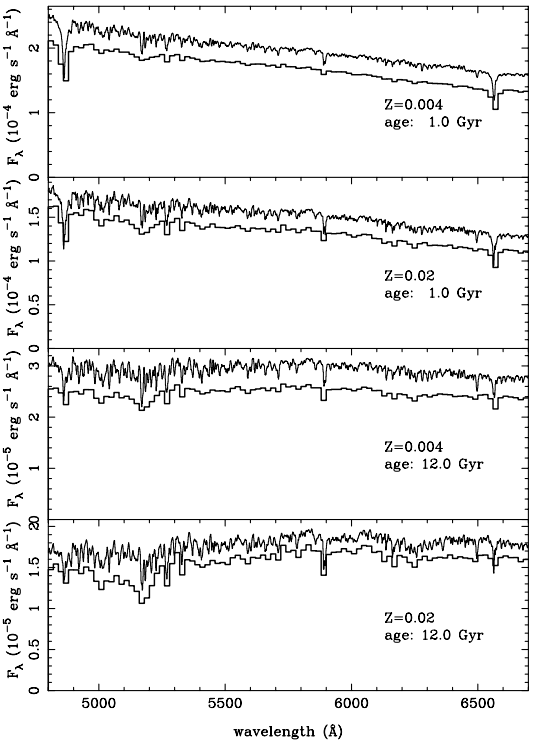

Fig. 9. Synthetic spectra built with STELIB compared to synthetic spectra obtained with Kurucz spectra using GISSEL02. SSP, wavelength range 4800Å to 7000Å, Z=0.02 (solar metallicity) and Z=0.004, from 1 Gyr to 12 Gyr. The Kurucz spectra are shifted downward by 10% of the scale for clarity.

Cenarro, A. J., Cardiel, N., Gorgas, J., et al. 2001, MNRAS 326, 959

di Benedetto, G. P. 1998, A&A 339, 858

Fioc, M., & Rocca-Volmerange, B. 1997, A&A 326, 950

Guiderdoni, B., & Rocca-Volmerange, B. 1987, A&A 186, 1

Gunn, J. E., & Stryker, L. L. 1983, ApJS 52, 121

Hamuy, M., Walker, A. R., Suntzeff, N. B., et al. 1992, PASP 104, 533

Hamuy, M., Suntzeff, N. B., Heathcote, S. R., et al. 1994, PASP 106, 566

Hayes, D. S. 1970, ApJ 159, 165

Hayes, D. S. 1985, in "Calibration of fundamental stellar quantities"; Proceedings of the Symposium, Como, Italy, May 24-29 1984, Dordrecht, D. Reidel Publishing Co., p. 225

Høg, E., Fabricius, C., Makarov, V. V., et al. 2000, A&A 355, L27

Johnson, H. L. 1980, Rev. Mex. Astron. Astrofis. 5, 25

Jones, L.A. 1997, Ph.D. Thesis, University of North Carolina at Chapel Hill

Katz, D., Soubiran, C., Cayrel, R., Adda, M. & Cautain, R. 1998, A&A 338, 151

Kurucz, R. L. 1992, IAU Symp. 149: "The Stellar populations of Galaxies", B. Barbuy and A. Renzini eds, Kluwer Academic Publishers, p225

Kroupa, P. 2001, MNRAS 322, 231

Lançon, A., & Rocca-Volmerange, B. 1992, A&AS 96, 593

Lejeune, T., Cuisinier, F., & Buser, R. 1997, A&AS 125, 246

Lejeune, T., Cuisinier, F., & Buser, R. 1998, A&AS 130, 75

Mermilliod, J.-C., Mermilliod, M., & Hauck, B. 1997, A&AS 124, 349

Montes, D., Ramsey, L. W., & Welty, A. D. 1999, ApJS 123, 283
Oke, J. B. 1990, AJ 99, 1621
Pelat, D. 1997, MNRAS 284, 365
Perryman, M. A. C., Lindegren, L., Kovalevsky, J., et al. 1997, A&A 323, L49
Pickles, A. J. 1998, PASP 110, 863
Prugniel, P. & Soubiran, C. 2001, A&A 369, 1048
Schaller G., Schaerer D., Meynet G., & Maeder A. 1992, A&AS 96, 269
Treu, T., Stiavelli, M., Bertin, G., Casertano, S., & Møller, P. 2001, MNRAS 326, 237
Westera, P., Lejeune, T., Buser, R., Cuisinier, F., & Bruzual, G. 2002, A&A 381, 524
Whiteoak, J. B 1966, ApJ 144, 305

Appendix A: Synthetic photometry and photometric reliability of STELIB

We present in this section a detailed comparison between the synthetic photometry derived for the STELIB library and the Lausanne database (Mermilliod et al. 1997). Magnitudes for STELIB stars have been obtained using the flux calibrated spectra without any correction for dereddening or radial velocity. The photometric bands are UBVRI, with filter transmissions as close as possible to the Johnson filters commonly used in the Lausanne database. Table A.1 summarizes the characteristics of the different filters.

Tables A.3 to A.6 provide with the UVBRI synthetic photometry for most of STELIB stars, together with the photoelectric photometry coming from the Lausanne database. Stars known to be variable or for which the spectrum is incomplete in a given filter have been discarded from this analysis. Almost all stars in this library have UBV Johnson magnitudes available, whereas R and I magnitudes are available only for 70% of the whole sample. In addition, magnitudes in the R and I bands are given either in the Johnson system or in the Eggen or Cousins systems. The later are identified by a comment in the last column of Tables A.3 to A.6. When a filter band is missing in the STELIB spectra, the corresponding magnitude is given by "-" in the tables. A small extrapolation up to ∼100Å is allowed in U and I when needed, towards the blue and the red edges of the filters. The following caveats apply in the comparison of photoelectric with synthetic magnitudes derived from our spectra:

- The effective filter transmissions in the different bands could be different between the photoelectric and the synthetic magnitudes.
- The transmission of the Johnson U band has been set to zero in our calculations for wavelengths shorter than 3200Å, which corresponds to the blue limit of the STELIB spectra.
- Although the majority of stars in the Lausanne database are given in the Johnson system, STELIB spectra do not cover completely the standard I band. Thus, the effective transmission in the I band has been adapted to the red limit of our spectra in wavelength. When spectra extend up to ∼9800Å, we use the broadest and redest version of the I band filter, identified by I in Table A.1, which is closer (although not identical) to a true Johnson filter. For spectra with red wavelegth limits bluer than ∼9800Å, we used the I Cousins filter instead, identified by $I_{Cousins}$ in Table A.1.

Table A.1. Characteristics of filters used in Appendix A: the effective wavelength $\lambda_{\rm eff}$ and the band width.

Filter	$\lambda_{\rm eff}$ [Å]	width [Å]
U	3594	377
B	4462	742
V	5554	736
R	6939	1507
I	8548	1307
$I_{Cousins}$	8060	924

Table A.2. Dispersion values in the comparison between synthetic magnitudes and photoelectric photometry from the Lausanne database

quantity	rms	quantity	rms
ΔU	0.145	$\Delta U-B$	0.156
ΔB	0.044	$\Delta B-V$	0.083
ΔV	0.072	$\Delta V-R$	0.135
ΔR	0.172	$\Delta R-I$	0.177
ΔI	0.249		

These stars are identified by an asterisk in Tables A.3 to A.6.

Figures A.1 to A.3 display the residuals of the comparison between synthetic photometry and the published Lausanne database. Table A.2 summarizes the dispersion values obtained in the different filters and colors. As expected, the smallest dispersions correspond to the B and V magnitudes and B-V colors, for which we have the highest degree of confidence in the correspondance between filter bands. For these 2 filters, the rms dispersion is quite consistent with the photometric accuracy derived from standard stars. The dispersion is much higher in the I band, as expected taking into account the inhomogeneities both in the photometric systems and the wavelegth coverage for the different objects. The situation in the U and R bands are intermediate. The wavelegth coverage could be responsible for the dispersion in U, (where the photometric systems are more consistent than in I), whereas the culprit in R is more likely the photometric system, but this point is difficult to assess. According to figures A.1 to A.3, there is no obvious color trend in the residuals neither in magnitude nor in color, except for the R-I and maybe in V-R in Figure A.3. This color trend is due to a residual difference between the filters used to compute synthetic magnitudes and the true Johnson filter. On the other hand, the relatively small dispersion in the R-I residuals as compared to the corresponding dispersion in R and I magnitudes (Figure A.3) indicates that the two photometric systems used are both internally consistent, but different from each other.

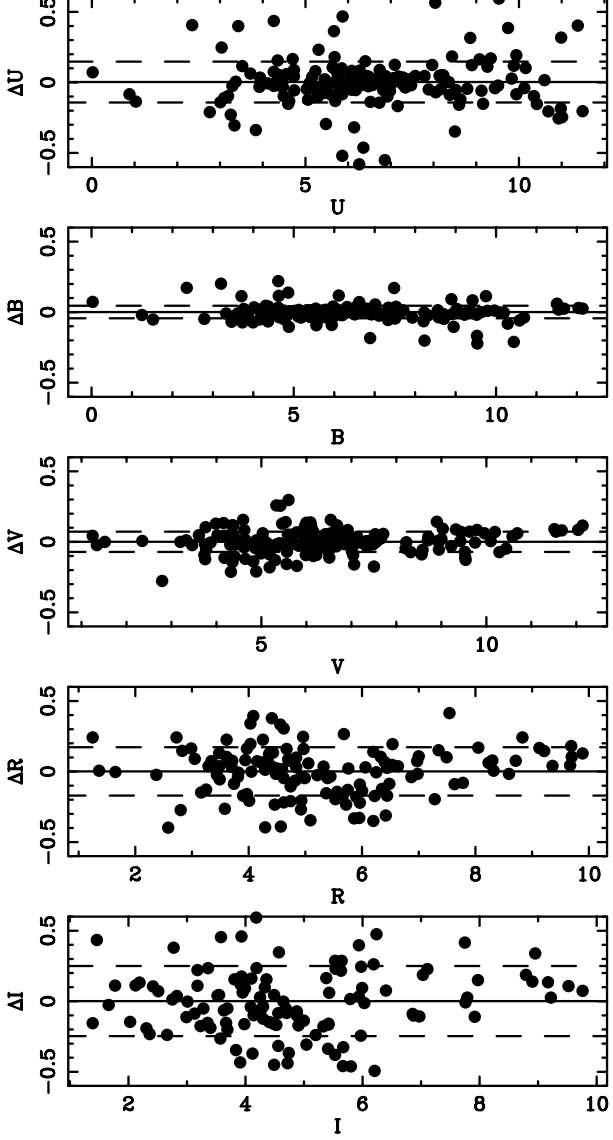

Fig. A.1. Residuals of the comparison between synthetic photometry and published photoelectric photometry: UBVRI magnitude residuals versus Johnson magnitudes in the Lausanne database. Dashed lines correspond to 1 σ rms.

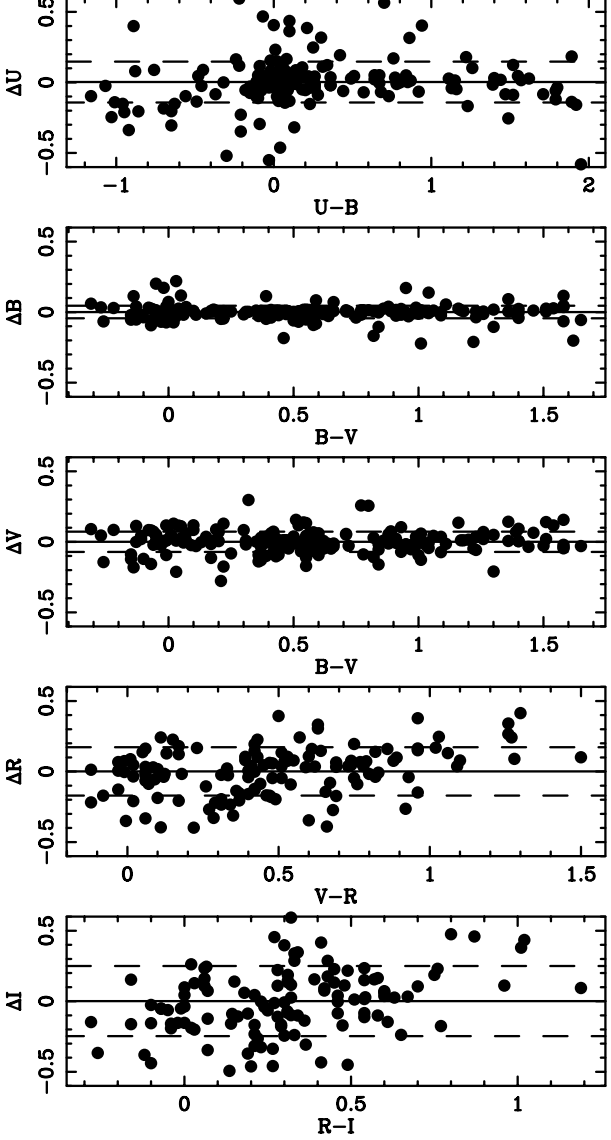

Fig. A.2. Residuals of the comparison between synthetic photometry and published photoelectric photometry: UBVRI magnitude residuals versus Johnson colors in the Lausanne database. Dashed lines correspond to 1 σ rms.

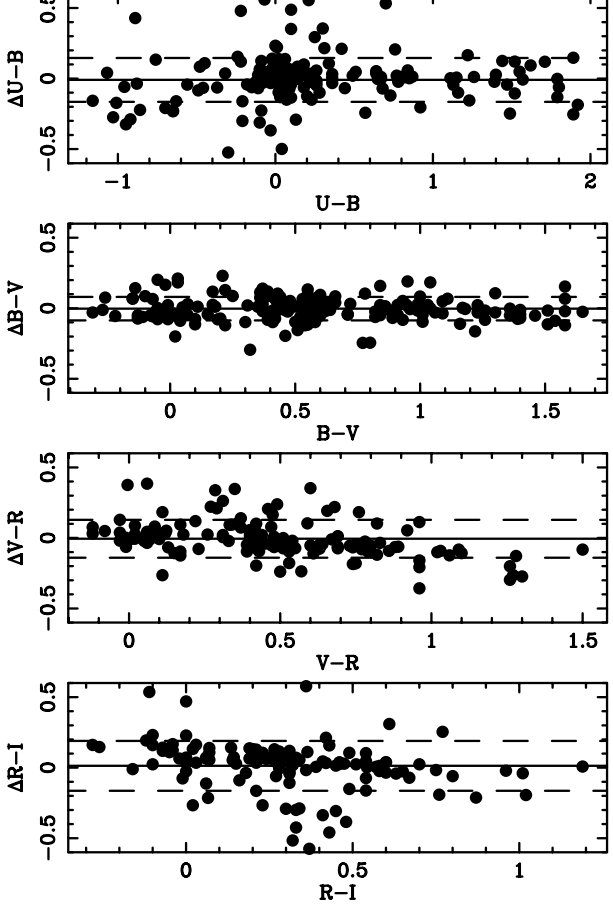

Fig. A.3. Residuals of the comparison between synthetic photometry and published photoelectric photometry: color residuals versus Johnson colors in the Lausanne database. Dashed lines correspond to 1 σ rms.

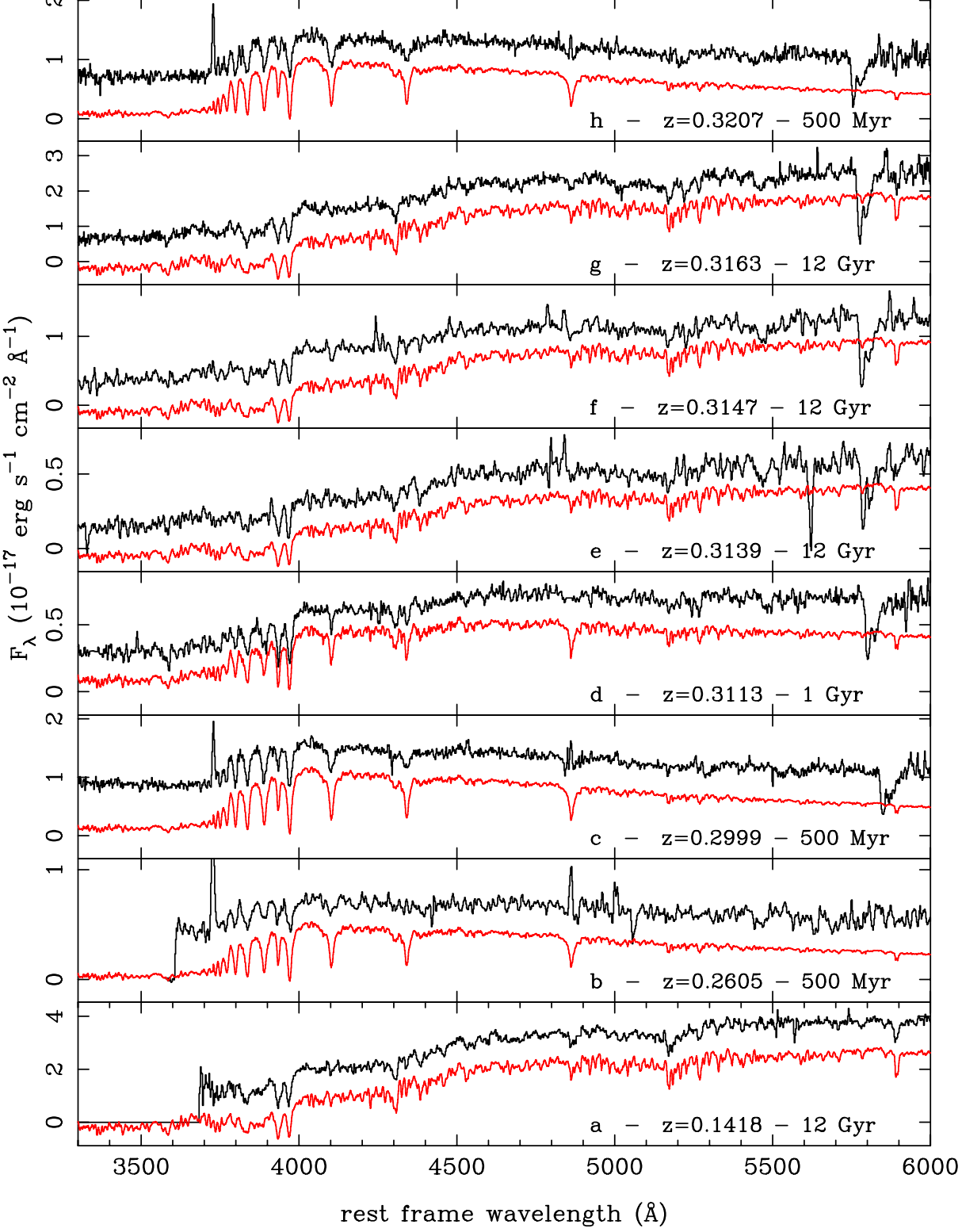

Fig. 10. Comparison of galaxy spectra, in and foreground of the cluster of galaxies AC114, with solar metallicity SSP synthetic spectra. See Table 12 for identification. The observed spectra are not corrected for atmospheric molecular bands (the main one appears at about 5800Å for z∼0.3 galaxies)). The observed spectra appear as a black line, and the model as a grey line. The model spectra are shifted downward by 20% of the scale for clarity. The legends in the figure give the observed redshift of the galaxies and the age of the models. The contribution of emission lines in the Balmer series is visible on observed spectra b, c and h.

	photoelectric photometry					synthetic photometry from spectra					
Star	U	B	V	R	I	U	B	V	R	I	comment
HD 2857	10.42	10.19	9.99	-	-	10.27	10.19	10.06	9.92	9.80	
HD 6268	9.26	8.95	8.11	-	-	9.37	8.85	8.06	7.45	7.02	
HD 15318	4.12	4.23	4.28	4.26	4.31	4.11	4.24	4.32	4.31	4.31	*
HD 21581	9.74	9.53	8.71	7.97	7.43	10.13	9.36	8.60	8.05	7.64	
HD 26630	5.75	5.11	4.15	3.36	2.82	5.77	5.08	4.13	3.43	3.12	*
HD 30614	3.43	4.32	4.29	4.18	4.18	3.83	4.29	4.08	3.78	3.38	
HD 30739	4.35	4.37	4.36	4.30	4.30	4.51	4.38	4.41	4.33	4.32	
HD 32034	9.16	9.79	9.69	9.52	9.46	9.01	9.80	9.77	9.70	9.63	*
HD 32923	5.71	5.57	4.92	4.65	4.42	5.80	5.57	4.87	4.38	4.48	* Eggen
HD 33579	9.08	9.32	9.13	8.90	8.75	9.24	9.33	9.22	9.07	8.95	*
HD 34411	5.45	5.33	4.71	4.18	3.86	5.47	5.33	4.69	4.26	4.51	*
HD 34816	3.01	4.02	4.29	4.41	4.69	2.87	4.05	4.33	4.42	4.60	
HD 35497	1.03	1.52	1.65	1.66	1.76	0.89	1.47	1.65	1.66	1.79	*
HD 36512	3.29	4.36	4.62	4.74	5.00	3.26	4.29	4.48	4.52	4.70	*
HD 36673	3.04	2.79	2.58	2.36	2.15	3.29	2.74	2.30	1.96	1.98	*
HD 37394	7.57	7.06	6.22	5.53	5.10	7.62	7.06	6.06	5.36	5.45	*
HD 37828	8.86	8.00	6.87	5.94	5.27	9.18	-	-	5.90	5.36	
HD 38247	9.94	8.23	6.61	-	-	9.86	8.03	-	4.44	3.20	
HD 39587	5.06	4.99	4.40	3.89	3.58	4.94	4.99	4.40	3.93	3.79	
HD 39866	7.18	6.92	6.62	-	-	7.22	6.90	6.70	6.47	6.50	*
HD 39949	-	8.32	7.23	-	-	9.09	8.30	7.16	6.50	6.80	*
HD 40111	3.84	4.76	4.82	4.76	4.87	3.50	4.71	4.80	4.70	4.33	
HD 41636	8.23	7.39	6.35	-	-	8.28	7.38	6.34	5.65	4.98	
HD 41667	10.10	9.54	8.53	-	-	-	9.32	8.40	7.75	7.28	
HD 42454	9.34	8.58	7.35	6.39	5.70	9.51	8.54	7.29	6.54	-	*
HD 43153	4.73	5.18	5.33	-	-	4.82	5.16	5.24	5.23	5.32	*
HD 45829	9.83	8.21	6.63	5.54	4.78	9.86	8.14	6.58	5.58	5.07	*
HD 46223	6.74	7.50	7.28	6.97	6.81	6.83	7.45	7.10	6.77	6.76	*
HD 47129	5.23	6.11	6.06	5.97	5.91	5.31	6.23	6.17	6.00	6.22	*
HD 47731	8.36	7.51	6.42	6.07	5.71	8.36	7.51	6.46	5.76	4.88	Eggen
HD 48329	5.86	4.39	2.99	2.03	1.42	5.78	4.35	2.99	2.19	1.33	
HD 48682	5.85	5.79	5.24	-	-	5.95	5.75	5.07	4.56	4.34	
HD 49933	6.05	6.15	5.76	-	-	6.10	6.13	5.66	5.26	5.13	*
HD 52005	9.12	7.33	5.68	4.42	3.59	9.06	7.27	5.65	4.69	-	*
HD 53929	5.51	5.97	6.10	-	-	5.48	6.01	6.21	6.21	6.28	
HD 54719	7.07	5.67	4.41	3.45	2.82	7.10	5.67	4.43	3.83	-	
HD 58551	-	7.00	6.54	6.12	5.81	6.87	6.99	6.54	6.31	-	
HD 59881	5.64	5.46	5.24	-	-	5.75	5.47	5.37	5.31	5.72	*
HD 60178	-	-	-	-	-	2.11	2.03	1.50	0.63	-	
HD 60778	9.44	9.22	9.11	-	-	9.40	9.20	9.08	8.94	9.13	
HD 61064	5.67	5.57	5.13	-	-	6.03	5.58	5.06	4.78	5.16	
HD 63077	5.87	5.94	5.36	-	-	6.34	5.85	5.37	4.96	4.68	
HD 64090	8.79	8.92	8.30	7.75	7.34	8.75	8.91	8.31	7.83	7.82	*
HD 65583	7.89	7.71	7.00	6.40	5.98	7.84	7.72	7.06	6.51	6.12	
HD 67767	6.98	6.54	5.72	5.41	5.14	6.92	6.55	5.75	5.18	4.87	* Eggen
HD 69897	5.54	5.60	5.14	-	-	5.54	5.60	5.13	4.72	4.52	
HD 72184	8.17	7.01	5.90	5.43	5.03	8.12	7.06	5.89	5.25	5.69	* Eggen
HD 72324	8.25	7.38	6.35	5.93	5.58	8.26	7.38	6.33	5.81	-	*
HD 74739	5.82	5.04	4.03	3.28	2.79	5.81	5.04	4.05	3.48	3.76	*
HD 75732	7.46	6.81	5.95	5.66	5.40	7.48	6.83	5.96	5.34	5.00	*
HD 76151	6.88	6.66	6.00	5.64	5.31	6.92	6.67	5.97	5.50	5.66	* Cousins
HD 76943	4.44	4.40	3.97	3.57	3.35	4.45	4.40	3.87	3.41	3.15	*

Table A.3. Photometry of STELIB stars from Lausanne database and synthetic photometry from spectra

Star	photoelectric photometry U	B	V	R	I	synthetic photometry from spectra U	B	V	R	I	comment
HD 77350	5.29	5.40	5.44	5.42	5.46	5.19	5.37	5.43	5.38	5.36	
HD 77729	10.60	9.03	7.63	6.87	6.29	10.62	9.05	7.72	6.78	6.25	* Eggen
HD 78418	6.82	6.62	5.96	5.67	5.44	6.77	6.69	5.95	5.45	5.18	* Eggen
HD 79158	4.70	5.18	5.32	-	-	4.75	5.14	5.14	4.97	4.86	
HD 79452	7.20	6.84	6.00	-	-	7.24	6.84	5.98	5.37	4.90	
HD 80081	3.92	3.87	3.81	3.69	3.66	3.89	3.85	3.81	3.65	3.52	*
HD 81192	8.05	7.48	6.53	5.79	5.25	7.98	7.65	6.51	5.84	5.33	
HD 81809	6.14	6.01	5.37	5.00	4.64	5.82	5.98	5.36	4.85	4.56	* Cousins
HD 82210	5.67	5.34	4.57	3.91	3.50	-	5.32	-	3.52	3.13	*
HD 83632	10.93	9.44	8.05	7.03	6.28	10.68	9.43	8.12	7.20	6.53	
HD 84937	8.50	8.71	8.32	7.92	7.64	8.15	8.66	8.36	7.92	7.59	
HD 85235	4.70	4.62	4.59	4.49	4.49	4.87	4.84	4.60	4.51	4.59	
HD 86728	6.28	6.02	5.37	-	-	6.26	6.03	5.34	4.79	4.41	
HD 87141	6.27	6.23	5.75	-	-	6.35	6.24	5.70	5.26	4.95	
HD 87696	4.73	4.66	4.48	4.30	4.23	4.77	4.68	4.49	4.28	4.17	
HD 87737	3.25	3.46	3.49	3.40	3.38	3.02	3.39	3.47	3.35	3.25	
HD 87822	6.69	6.68	6.24	-	-	6.70	6.69	6.22	5.80	5.53	
HD 87901	0.88	1.25	1.36	1.39	1.49	0.80	1.23	1.40	1.40	1.40	
HD 88355	6.92	6.90	6.44	6.03	5.76	6.82	6.90	6.45	6.06	5.81	
HD 88609	9.94	9.52	8.59	7.79	7.16	10.13	9.50	8.52	7.77	7.25	
HD 89025	3.94	3.75	3.44	3.13	2.94	3.97	3.75	3.42	3.11	2.91	
HD 89254	5.70	5.60	5.28	-	-	5.57	5.60	5.58	5.52	5.56	
HD 89758	6.52	4.63	3.05	1.77	0.81	6.38	4.75	3.01	1.86	0.98	
HD 90277	5.16	4.99	4.74	4.48	4.34	5.20	4.99	4.66	4.37	4.24	*
HD 90508	7.09	7.04	6.44	5.97	5.67	7.21	7.04	6.35	5.80	5.49	*
HD 90537	5.76	5.12	4.21	3.52	3.06	5.81	5.13	4.20	3.59	3.16	
HD 91316	2.76	3.71	3.85	3.89	4.05	2.55	3.82	-	-	4.26	
HD 92769	5.77	5.68	5.51	-	-	5.77	5.69	5.49	5.28	5.11	
HD 93250	-	-	-	-	-	6.54	7.53	7.41	7.15	7.03	
HD 93430	-	-	-	-	-	10.01	10.05	9.57	9.16	8.85	
HD 93765	6.40	6.43	6.06	-	-	6.43	6.43	6.03	5.68	5.46	
HD 94028	8.52	8.70	8.23	7.76	7.46	8.47	8.69	8.24	7.82	7.51	
HD 94247	7.97	6.45	5.09	4.49	4.00	8.09	6.45	5.10	4.14	3.61	* Eggen
HD 94264	5.78	4.86	3.82	2.99	2.45	5.72	5.00	3.78	2.98	2.40	
HD 95345	7.11	6.00	4.84	4.25	3.71	7.14	6.02	4.98	4.28	3.80	Cousins
HD 95418	2.35	2.35	2.37	2.31	2.35	2.76	2.52	2.38	2.29	2.22	
HD 95735	10.13	9.00	7.49	5.99	4.80	10.09	9.00	7.51	6.09	4.95	
HD 97633	3.37	3.33	3.34	3.35	3.35	3.37	3.32	3.35	3.42	3.26	
HD 97916	9.51	9.63	9.21	8.79	8.48	9.49	9.63	9.28	8.94	8.73	
HD 98262	6.43	4.88	3.48	2.42	1.72	6.48	4.88	3.49	2.55	1.89	
HD 98839	6.79	5.99	4.99	4.24	3.78	6.79	5.98	4.90	4.19	3.76	
HD 99028	4.42	4.35	3.94	3.55	3.34	4.39	4.37	3.97	3.63	3.45	
HD 99747	6.14	6.22	5.86	-	-	6.15	6.20	5.77	5.34	5.04	
HD 100006	7.41	6.59	5.53	5.04	4.68	7.43	6.60	5.57	4.84	4.43	* Eggen
HD 100889	4.47	4.62	4.70	4.69	4.76	4.44	4.65	4.78	4.78	4.77	*
HD 101501	6.30	6.04	5.32	4.70	4.39	6.29	6.04	5.29	4.74	4.37	
HD 101606	6.08	6.19	5.75	5.33	5.04	6.08	6.17	5.66	5.20	4.92	*
HD 102212	7.34	5.54	4.03	2.77	1.76	7.30	5.57	4.17	3.11	2.20	
HD 102224	6.04	4.89	3.71	2.83	2.23	6.05	4.90	3.72	2.91	2.33	
HD 102634	6.73	6.66	6.14	-	-	6.59	6.67	6.26	5.93	5.74	
HD 102870	4.26	4.16	3.61	3.18	2.90	4.70	4.11	3.65	3.28	3.07	*
HD 102870	4.26	4.16	3.61	3.18	2.90	4.24	4.18	3.74	3.41	3.18	*

Table A.4. Photometry of STELIB stars from Lausanne database and synthetic photometry from spectra (cont'd)

	photoelectric photometry					synthetic photometry from spectra					
Star	U	B	V	R	I	U	B	V	R	I	comment
HD 104893	11.38	10.44	9.22	-	-	11.78	10.23	9.17	8.39	7.78	
HD 105546	-	-	-	-	-	9.28	9.04	8.22	7.54	7.04	
HD 106038	-	-	-	-	-	10.15	10.26	9.67	9.12	8.75	
HD 107213	7.01	6.93	6.40	-	-	7.00	6.94	6.40	5.97	5.70	
HD 108177	9.88	10.10	9.67	9.22	8.90	10.00	10.10	9.68	9.27	8.99	
HD 109995	7.79	7.66	7.61	-	-	7.84	7.66	7.63	7.51	7.40	
HD 110897	6.47	6.51	5.96	5.42	5.13	6.44	6.50	5.85	5.33	5.03	*
HD 111028	7.43	6.65	5.66	5.20	4.87	7.43	6.67	5.70	5.03	4.69	* Eggen
HD 112033	-	-	-	-	-	10.76	10.51	9.85	9.30	8.91	
HD 113022	6.63	6.63	6.20	6.21	6.07	6.64	6.64	6.22	5.85	5.64	* Eggen
HD 113139	5.31	5.30	4.93	4.56	4.35	5.54	5.31	4.80	4.36	4.09	*
HD 113226	4.49	3.76	2.83	2.19	1.74	4.39	3.78	2.93	2.34	1.93	
HD 113337	6.48	6.49	6.07	-	-	6.52	6.49	6.00	5.62	5.38	
HD 114330	4.37	4.37	4.38	4.33	4.33	4.42	4.41	4.50	4.47	4.49	*
HD 115383	5.89	5.79	5.21	4.88	4.57	5.90	5.81	5.28	4.85	4.56	Cousins
HD 116842	4.26	4.18	4.01	3.84	3.77	4.34	4.18	3.90	3.63	3.48	*
HD 117176	5.94	5.68	4.97	4.36	3.97	5.90	5.69	5.02	4.52	4.19	
HD 120136	5.03	4.98	4.50	4.09	3.85	4.98	4.99	4.51	4.11	3.87	
HD 122408	4.47	4.35	4.25	4.10	4.04	4.51	4.36	4.37	4.33	4.26	
HD 122563	7.47	7.11	6.20	5.38	4.80	7.45	7.09	6.22	5.52	5.03	
HD 123299	3.52	3.61	3.66	3.69	3.76	3.64	3.60	3.71	3.76	3.77	
HD 124425	6.40	6.38	5.91	-	-	6.55	6.39	5.92	5.55	5.32	
HD 124570	6.18	6.09	5.55	-	-	6.13	6.11	5.69	5.31	5.05	
HD 124850	4.62	4.59	4.08	3.58	3.31	4.49	4.59	4.24	3.97	3.83	
HD 125560	7.46	6.07	4.84	3.95	3.35	7.44	6.08	4.88	4.05	3.47	
HD 126141	6.57	6.60	6.23	-	-	6.55	6.61	6.24	5.90	5.64	
HD 126660	4.56	4.55	4.05	3.63	3.38	4.62	4.55	4.04	3.63	3.38	
HD 127665	6.32	4.88	3.58	2.66	2.01	6.34	4.78	3.37	2.40	1.83	*
HD 128167	4.74	4.82	4.46	4.12	3.93	4.68	4.79	4.32	3.89	3.62	*
HD 130109	3.71	3.73	3.74	3.67	3.69	3.77	3.66	3.65	3.58	3.60	
HD 130948	6.43	6.42	5.86	5.80	5.60	6.46	6.44	5.91	5.47	5.20	* Eggen
HD 131156	5.61	5.33	4.56	3.93	3.50	5.52	5.34	4.82	4.26	3.74	
HD 132142	8.90	8.56	7.78	7.11	6.66	9.02	8.57	7.69	7.03	6.95	
HD 134083	5.33	5.36	4.93	4.53	4.32	5.29	5.36	4.90	4.49	4.21	
HD 134169	8.14	8.22	7.69	-	-	8.19	8.22	7.69	7.21	6.93	
HD 135722	5.10	4.43	3.48	2.75	2.24	5.10	4.43	3.46	2.79	2.31	
HD 136512	7.29	6.52	5.51	-	-	7.32	6.53	5.57	4.89	4.40	
HD 137759	5.68	4.46	3.29	2.51	1.91	5.86	4.47	3.30	2.55	2.04	
HD 138290	6.87	6.93	6.56	-	-	6.89	6.94	6.59	6.26	6.04	
HD 139641	6.64	6.15	5.26	-	-	6.67	6.16	5.33	5.64	4.48	
HD 139669	8.43	6.54	4.96	3.93	3.06	8.61	6.58	5.12	4.18	3.58	Eggen
HD 139798	6.09	6.11	5.76	5.43	5.25	6.17	6.12	5.76	5.45	5.37	
HD 141004	5.13	5.03	4.43	3.92	3.60	5.11	5.04	4.49	4.05	3.78	
HD 141714	5.78	5.42	4.62	3.99	3.57	5.76	5.43	4.88	4.29	3.72	
HD 142373	5.19	5.18	4.62	4.14	3.82	5.15	5.17	4.58	4.09	3.78	
HD 144206	4.32	4.64	4.74	4.72	4.82	4.32	4.60	4.62	4.51	4.44	*
HD 145675	8.20	7.53	6.65	-	-	8.25	7.57	6.70	6.07	5.72	
HD 145976	6.85	6.90	6.52	-	-	6.90	6.91	6.55	6.21	5.97	
HD 146051	6.26	4.31	2.73	1.46	0.44	5.68	4.36	2.71	1.70	0.94	
HD 147394	3.19	3.75	3.90	3.98	4.14	3.09	3.70	3.78	3.81	4.04	
HD 148513	8.63	6.84	5.38	4.56	4.02	8.51	6.85	5.44	4.52	4.00	Eggen
HD 149121	5.44	5.59	5.64	-	-	5.37	5.56	5.69	5.65	5.59	

Table A.5. Photometry of STELIB stars from Lausanne database and synthetic photometry from spectra (cont'd)

	photoelectric photometry					synthetic photometry from spectra					
Star	U	B	V	R	I	U	B	V	R	I	comment
HD 150275	8.04	7.34	6.35	-	-	8.61	7.37	6.36	5.66	5.23	
HD 151044	7.03	7.01	6.48	6.04	5.78	7.04	7.01	6.41	5.95	-	
HD 151217	8.60	6.68	5.14	-	-	8.44	6.71	5.26	4.15	2.30	
HD 154733	8.38	6.86	5.56	4.90	4.43	8.29	6.88	5.61	4.76	4.32	* Eggen
HD 155646	7.17	7.13	6.64	-	-	-	-	6.63	6.27	-	
HD 156283	6.27	4.60	3.16	2.20	1.48	-	-	3.12	2.05	-	
HD 157089	7.53	7.55	6.97	6.45	6.10	-	-	6.97	6.52	-	
HD 157214	6.08	6.01	5.39	4.88	4.54	6.03	6.00	5.34	4.83	4.50	
HD 157373	6.72	6.82	6.41	-	-	-	-	6.41	6.06	5.98	*
HD 157856	6.86	6.89	6.43	-	-	6.31	6.71	6.44	-	-	
HD 157881	10.16	8.90	7.54	6.24	5.44	10.26	8.99	7.68	6.65	5.98	
HD 157999	7.43	5.83	4.33	3.23	2.46	-	-	4.30	3.31	2.35	*
HD 159181	4.40	3.77	2.80	2.12	1.64	-	-	2.75	1.85	1.81	
HD 159332	6.15	6.15	5.66	-	-	-	-	5.66	8.62	-	
HD 160693	8.92	8.95	8.37	7.89	7.55	-	-	8.37	-	-	
HD 161817	7.27	7.13	6.98	6.86	6.71	7.26	7.12	7.02	6.84	6.69	Cousins
HD 163993	5.32	4.64	3.70	3.01	2.55	5.25	4.64	3.67	3.04	2.61	
HD 164349	7.16	5.93	4.67	3.81	3.24	6.99	5.92	4.74	3.97	3.46	
HD 164353	3.34	3.99	3.97	3.91	3.88	3.04	3.92	4.10	4.07	4.07	*
HD 165908	5.48	5.57	5.05	4.57	4.23	5.19	5.50	5.04	4.63	4.64	*
HD 166285	6.08	6.12	5.68	-	-	-	-	5.68	5.35	5.33	*
HD 166620	7.87	7.28	6.40	5.63	5.14	-	-	6.39	5.70	5.42	*
HD 167858	6.95	6.93	6.62	-	-	-	-	6.63	6.35	5.63	
HD 172167	0.02	0.03	0.03	0.07	0.10	0.09	0.10	-	-	-	
HD 173780	7.26	6.03	4.83	3.95	3.34	-	-	4.85	-	-	
HD 173880	4.56	4.49	4.36	4.19	4.13	-	-	4.36	4.31	4.43	*
HD 175305	8.08	7.93	7.18	6.53	6.04	-	7.89	-	-	-	*
HD 175640	5.86	6.16	6.21	-	-	5.34	6.16	6.21	6.15	6.18	
HD 176437	3.10	3.20	3.25	3.28	3.29	2.99	3.40	3.25	3.15	3.30	*
HD 181470	6.17	6.25	6.26	-	-	-	-	6.27	6.18	6.39	*
HD 182101	6.75	6.78	6.33	5.94	5.64	-	-	6.34	6.04	6.10	*
HD 182490	6.36	6.32	6.25	6.19	6.17	5.90	6.36	6.26	6.19	6.49	*
HD 184960	6.19	6.20	5.73	5.27	4.99	-	-	5.74	-	-	
HD 185657	8.21	7.46	6.46	-	-	-	-	6.45	-	-	
HD 188209	4.60	5.56	5.63	5.53	5.65	4.45	5.47	5.47	5.34	5.33	
HD 188510	9.31	9.42	8.83	8.26	7.89	-	9.50	8.84	8.50	8.77	
HD 195725	4.57	4.41	4.21	4.04	3.95	-	-	4.22	-	-	
HD 195986	5.91	6.48	6.59	-	-	-	-	6.61	-	-	
HD 197345	1.11	1.34	1.25	1.14	1.04	-	-	1.23	1.38	-	
HD 268623	10.69	11.55	11.61	-	-	10.49	11.57	11.68	11.70	11.76	
HD 268749	11.49	12.14	12.10	-	-	11.29	12.17	12.21	12.17	12.18	
HD 268819	10.97	10.58	10.08	-	-	-	10.52	10.12	9.83	9.61	
HD 269697	10.99	10.69	10.28	-	-	11.31	10.65	10.34	10.12	9.93	
HD 269698	11.01	12.04	12.26	-	-	10.76	12.07	12.34	12.39	12.52	
HD 269781	-	9.96	9.89	9.76	9.69	9.21	9.97	9.95	9.89	9.82	*
HD 271163	10.98	11.68	11.75	-	-	10.80	11.70	11.83	11.84	11.91	
HD 271182	10.74	10.29	9.70	9.17	8.86	-	10.21	9.63	9.27	9.06	*
HD 338529	9.53	9.75	9.36	8.95	8.62	10.12	9.86	9.36	8.99	9.02	*
Feige110	10.35	11.51	11.82	-	-	10.25	11.57	11.91	12.04	12.27	
G319	-	-	-	-	-	13.17	12.71	12.58	12.47	12.35	
LTT4364	-	-	-	-	-	10.72	11.64	11.49	11.39	11.30	

Table A.6. Photometry of STELIB stars from Lausanne database and synthetic photometry from spectra (cont'd)